

Fullerenes

A. V. Eletskii and B. M. Smirnov

Kurchatov Institute Scientific Center, Russia; Institute of High Temperatures, Russian Academy of Sciences, Moscow

(Submitted 3 August 1992)

Usp. Fiz. Nauk **36**, 33–60 (February 1993)

Contemporary studies of fullerenes-carbon clusters as C_{60} , C_{70} , C_{76} , C_{84} etc., whose atoms are located on a spherical or ellipsoidal surface are reviewed. Fullerene structures, methods for producing them, processes involving fullerenes, and the production of fullerenes are considered. The properties of fullerites (carbon crystals consisting of fullerenes) and the properties of compounds are discussed.

(The English translation of this paper was reviewed and changed in numerous instances by the Authors.)

1. INTRODUCTION

The term "fullerenes" refers to closed molecules as C_{60} , C_{70} , C_{76} , and C_{84} , in which all the carbon atoms are located on a spherical or spheroidal surface. In these molecules the carbon atoms are positioned at the vertices of regular hexagons or pentagons, which cover the surface of the sphere or spheroid. The main fullerene is the C_{60} molecule, which is characterized by the highest symmetry and consequently the greatest stability among fullerenes. In this molecule, which is reminiscent of the covering of soccer ball and has the structure of a truncated regular icosahedron, the carbon atoms are distributed over the spherical surface at the vertices of 20 regular hexagons and 12 regular pentagons, so that every hexagon is bounded by three hexagons and three pentagons, and every pentagon is surrounded entirely by hexagons. Thus, every carbon atom in a C_{60} molecule is at the vertices of two hexagons and one pentagon, and is essentially indistinguishable from the other carbon atoms.

The term "fullerene" owes its origin to the name of the American architect Buckminster Fuller, who used similar structures in designing geodesic domes. For this reason the C_{60} molecule is often called Buckminsterfullerene, and carbon molecules having closed spherical or spheroidal configurations are called "fullerenes." In the American literature the abbreviated term "bucky-ball" is sometimes used. Fullerenes in the condensed state are called "fullerites," and doped fullerites are called "fullerides."

The possibility that stable C_{60} molecules having a closed spherical structure might exist was mentioned often in the literature long before the experimental observation of such a molecule^{1–5} (see also Ref. 6). However, the story of the present-day investigations began with the work of Kroto *et al.*,⁷ in which the C_{60} molecule was detected as a cluster containing a magic number of atoms. This served to initiate the studies of the various properties of this cluster.^{8–13} As a result of these investigations the closed spherical structure of the C_{60} molecule was reliably established, providing an explanation for its enhanced stability. It was also shown that the C_{70} molecule, which has the shape of a closed spheroid, exhibits enhanced stability.

The second stage in the study of fullerenes is associated with the creation in 1990 of a relatively simple efficient technology for producing fullerenes in macroscopic quantities.^{14–18} This technology permits graphite to be converted into C_{60} at a rate of about 1 g/h, which suffices to supply science studies and opens new possibility for production of new materials for industry. The efficiency with which C_{70} can be produced is about a factor of ten lower, but even this is enough for studies not only of thin films but also of polycrystals made from this type of molecule.

The technology product is a carbon deposit consisting of C_{60} with admixture of C_{70} and a small content of other fullerenes as C_{76} , C_{84} , C_{90} , C_{94} . The method of liquid chromatography developed recently allows to enrich a carbon deposit and to obtain samples consisting of fullerenes of each type. In spite of low productivities of this process for sparse fullerenes, this method opens new possibilities for the complete study of each fullerene separately.

Studies of fullerenes is a branch of science concerned with the investigation of molecules whose atoms are located on a closed surface. The development of this branch leads to production of materials with new properties. One of such materials is a superconductor which is a fullerene doped by atoms of alkali metals. This direction started in 1991^{19–22} gives a new group of superconductors whose critical temperature is the highest among molecular superconductors.

A number of review articles on fullerene investigations have been published previously.^{23–28} The present work is based on our previous review.²⁹ This review uses the same form, but contains a lot of new results, because during two years the state of the problems under consideration has changed remarkably. The aim of this review is to analyze the fullerene problem, to describe their properties and processes of their generation and detection. Besides, we would like to analyze the systems and processes involving fullerenes.

Making the analysis, we believe fullerenes to be simultaneously both clusters and molecules. Clusters and molecules are systems of bounded atoms. Molecules are more stable systems, i.e., attachment or release of one atom is

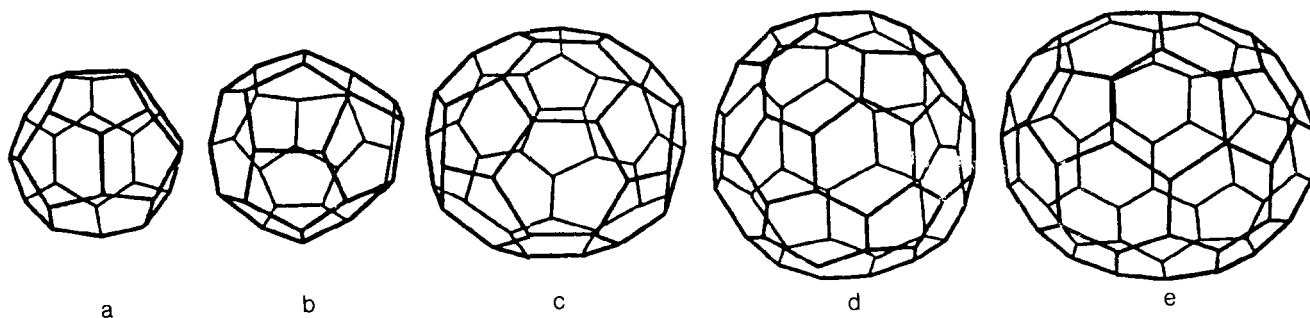


FIG. 1. Structure of fullerenes, consisting of pentagonal and hexagonal carbon rings. The number of C atoms in these is: a) 28; b) 32; c) 50; d) 60; e) 70 (Ref. 24). These numbers are magic for carbon clusters.

less probably for molecules than for clusters. Fullerenes are molecules in respect to processes of their generation and are molecules in respect to their structure. Because the difference between large molecules and clusters is not strong, we will not make the difference between these conceptions. Therefore we assume fullerenes to be simultaneously both clusters and molecules.

2. FULLERENES: AS CARBON CLUSTERS

2.1. C_{60} geometry

Structurally a C_{60} cluster is a truncated icosahedron. Let us examine this structure a little more closely in order to display its symmetry. An icosahedron¹⁰⁵ is a body whose surface consists of 20 regular triangles. Such a structure is exhibited by, e.g., a cluster containing 13 atoms of a noble gas.¹⁰⁶⁻¹⁰⁷ Let us construct an icosahedron. For this we choose one of the atoms as the center of a sphere, on which the remaining 12 atoms are located as follows. Two of them we put at the poles of the sphere, so that these two atoms lie on an axis passing through the center of the sphere. The other ten form two pentagons, whose planes are perpendicular to the specified axis. The vertices of the pentagons are displaced relative to one another by a rotation through an angle of $\pi/5$ in their circumscribed circles.

If we connect neighboring vertices on the sphere, then the resulting line segments form 20 regular triangles. This means that the distances between nearest neighbors on the sphere are identical, and each atom has five nearest neighbors on the sphere. The nearest neighbors to the atoms located at the poles are the atoms of the closer pentagon, while for each atom of a pentagon the nearest neighbors are two atoms of that pentagon, the two nearest atoms of the other pentagon, and the atom of the nearer pole.

It is important to note that the distance between nearest-neighbor atoms on the sphere differs somewhat from the radius of the sphere, i.e., from the distance between the central atom and the atoms on the sphere. Consequently, an icosahedron is not a close-packed structure, in which the atoms can be modeled by hard balls. In a close-packed structure the distances between arbitrary nearest neighbors are the same. Therefore, the icosahedron is modeled by soft balls.

Let us determine the relation between the icosahedron parameters, i.e., between the radius of the sphere on which the vertices of the icosahedron are located and the distance between nearest-neighbor vertices on the sphere. Figure 2 displays a cross section of the sphere made by a plane passing through the center, the icosahedron axis, and one vertex of each pentagon. This sketch shows the atoms in this plane, along with the notation used for the parameters in what follows. Let a be the distance between nearest-neighbor atoms on the sphere. We have the following relations, connecting these parameters. The side of a pentagon is equal to

$$a = 2r \sin(\pi/5). \quad (1)$$

The distance between nearest neighbors which are vertices of different pentagons is equal to

$$a = \{l^2 + [2r \sin(\pi/10)]^2\}^{1/2}. \quad (2)$$

Moreover, the distance between an atom at a pole and an atom in the nearest pentagon is equal to

$$a = \{[R - (l/2)]^2 + r^2\}^{1/2}. \quad (3)$$

In addition, as can be seen from the figure, we have the following relation among these parameters:

$$R^2 = r^2 + (l/2)^2. \quad (4)$$

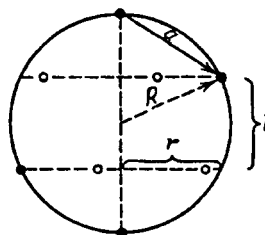


FIG. 2. Cross section of a sphere in which the vertices of an icosahedron are shown. The cross section is made by passing a plane through the center of the axis of the icosahedron and one vertex of each pentagon. The filled circles are the vertices of the icosahedron which lie on the plane in question, and the open circles are projections on this plane of the remaining vertices of the icosahedron. The figure is labeled with the distances used in the text.

As can be seen, three of these equations yield a relation among the parameters, while the fourth equation reproduces it, i.e., confirms the assumption that the distances between nearest-neighbor atoms on the sphere are identical. We use these equations to find the relations among the parameters. The first two equations yield $l=r$. Using the third equation we have the following relation among the parameters:

$$r=l=0.851a, \quad R=0.951a.$$

The fourth equation confirms these relations. As can be seen, the distance from the center to a vertex of the polyhedron is almost 5% less than the distance between neighboring vertices.

Now we pass from the icosahedron to the truncated icosahedron, which we obtain by drawing a new sphere about the center of symmetry. Since the icosahedron consists of 20 equilateral triangles formed by 30 line segments, all of the same length, and since each of these line segments intersects the sphere at two points, we have 30 points at which the sphere intersects the icosahedron. These intersection points correspond to the positions of the carbon atoms which compose a C_{60} cluster. The intersection points of the line segments belonging to the same vertex form pentagons, of which there are 12, i.e., equal to the number of vertices in the icosahedron. The line segments cut away by the sphere from the sides of the icosahedron are the sides of hexagons. Each triangle of the icosahedron gives one hexagon as a result of its crossing with the sphere. From this we find that the structure of the C_{60} cluster contains 20 hexagons, so that each one borders on three pentagons and 3 hexagons. Besides, 3 lines go out each vertex of the cluster. One of these is a common side of two hexagons, and two other ones are common sides of a pentagon and a hexagon.

The figure formed by carbon atoms of C_{60} has a high symmetry. Let us determine approximately the radius of the sphere on which the cluster atoms are located, accept that the side of a hexagon is equal to a . For this we cross the cluster with a plane which passes through its center and divides the cluster into symmetric parts. This plane cuts 4 hexagons and 4 pentagons in half and passes through two sides of a hexagon. The perimeter of the figure of intersection is equal to $10a+4b=16.16a$, where a is the side of the hexagon and $b=1.54a$ is the height of a pentagon. If we assume that the perimeter of the figure of intersection is equal to the circumference $2\pi R$ obtained by bisecting the sphere in which the cluster is inscribed, then the radius of the sphere is equal to $R=2.57a$. Replacing the straight line segments of the figure of intersection with arcs slightly increases the length of the circumference, which turns out to be equal to $16.46a$. Correspondingly, the radius of the sphere is equal to $R=2.62a$. Although this operation is not completely rigorous, since only the vertices of the figures are located on the surface of the sphere, the accuracy of this operation (better 1%) is enough for the analysis of C_{60} properties under consideration.

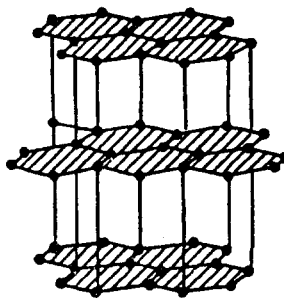


FIG. 3. Graphite structure.²⁸

2.2. Fullerene structure

Let us consider the chemical structure of fullerenes. A carbon atom has the electronic shell s^2p^2 . It provides the optimal chemical bond for pure carbon if each atom has 4 nearest neighbors with single bonds as it takes place in the diamond structure, or it has 3 nearest neighbors (the graphite structure). In the case of the graphite structure there are one double bond ($C=C$) and two single ($C-C$) bonds. Carbon clusters considered have the graphite structure, i.e., each atom has 3 nearest neighbors. The plane figure with such a structure consists of hexagons, the space figure consists of pentagons and hexagons. Fullerenes have the graphite chemical bonds and the closed surface. Therefore the surface formed by carbon atoms in fullerenes consists of pentagons and hexagons. Fig. 1 gives the sequence of such clusters.⁷

The fundamental element in fullerene structure is the hexagon, in the vertices of which the carbon atoms are located. Similar hexagons are also the fundamental structural element in graphite, shown in Fig. 3. Since the technology of production of fullerenes is based on thermal decomposition of graphite, it is natural to assume that hexagons of graphite become hexagons of fullerenes. Use it for the analysis of the fullerenes structure. Layers of graphite made up of regular hexagons with sides of length 0.142 nm are separated by a distance of 0.335 nm (Refs. 29, 30). Atoms of neighboring layers are located not one above the other, but shifted by half a lattice constant. Let us calculate the radius of the fullerene C_{60} , assuming that it is made up of graphite hexagons and using the model described above of a truncated icosahedron with identical sides. We take $R=2.62a=0.37$ nm, where a is the distance between nearest neighbors.

Fullerenes have two types of bonds: the single and the double carbon bonds. The single bond corresponds to the common side of a pentagon and hexagon, the double bond relates to common sides of two hexagons. Above we assumed that the system C_{60} has a high symmetry and lengths of all bonds are identical. According to experiments³²⁻³⁴ the lengths of single and double bonds do not coincide. They are equal 0.144 ± 0.001 nm for a single bond and 0.139 ± 0.001 nm for a double one respectively. Note that the length of the graphite bond 0.142 nm must be close to the length of common sides of hexagons in the cluster C_{60} . Besides, the hexagons making up the C_{60} struc-

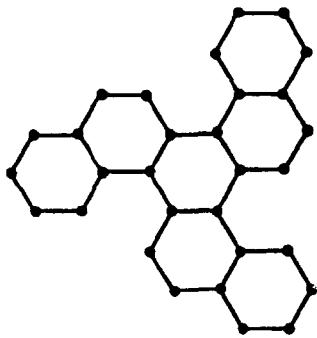


FIG. 4. Graphite fragment which might constitute half of the C_{60} fullerene.

ture differ somewhat from regular hexagons, and the estimate given above of the fullerene dimensions is only accurate to within 1–2%. A more accurate value for the radius of the C_{60} molecule, determined from x-ray analysis,¹⁸ is 0.357 nm.

The connection between graphite structure and the structure of a closed carbon cluster is discernible in the mechanism by which C_{60} clusters form from graphite. When graphite undergoes moderate heating, the bonds between neighboring layers are broken, and the vaporized layers break up into separate fragments. These fragments are a combination of hexagons, and the cluster is built up from them. One can expect that the C_{60} -cluster can be constructed from 10 hexagons combined in a closed structure. However it is impossible without cutting some hexagons. Indeed, there are not 10 hexagons in the C_{60} -structure which do not have common vertices with each other. Therefore, the C_{60} -structure is constructed by a more complicated way. For example, it can be constructed from 6 separate double hexagons with one common side.

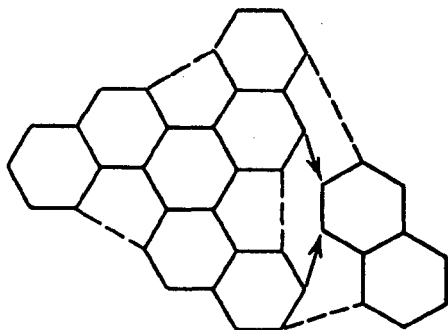


FIG. 5. The way of assembling of a part of a closed carbon molecule from graphite fragments. The joining of two fragments is shown. The large fragment, consisting of 7 hexagons (30 atoms) is bent into a three-dimensional structure, so that dashed lines match with the corresponding sides of a pentagon. Then the fragment consisting of two hexagons (10 atoms) forms a hexagon with the larger fragment (connections are shown by the arrows) and two pentagons (which match at dashed lines). Thus, from these fragments part of a C_{60} cluster is built up, consisting of 40 atoms and including 6 closed pentagons and 10 closed hexagons. The C_{60} fullerene can be obtained from this fragment by adding to it two more fragments which are double hexagons with 10 carbon atoms.²⁸

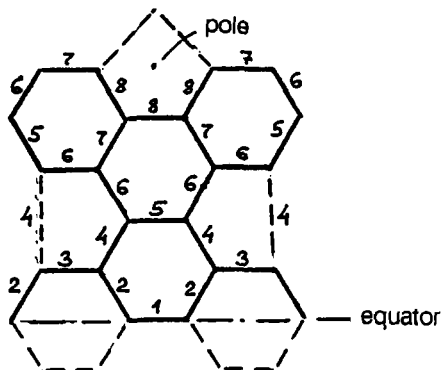


FIG. 6. Notations of bonds for the C_{70} -molecule according to Ref. 36. The development of a part of the C_{70} molecule is shown.

Each of these contains 10 atoms. This is probably the simplest choice. This approach can be modified if we assemble a cluster from fragments also consisting of double hexagons (Figs. 4 and 5). In particular, Fig. 4 shows one of these fragments. The C_{60} cluster in question consists of two fragments like that shown in the figure.

Note that, although the C_{60} molecule is characterized by two different types of C–C bond, all carbon atoms in this molecule are located in equivalent positions, so that each atom simultaneously belongs to two hexagons and one pentagon. Evidence for this comes from the nature of the nuclear magnetic resonance (NMR) spectrum of ^{13}C obtained by Taylor *et al.*,³⁵ which in the case of a sample of pure C_{60} consists of one resonance peak. In contrast, the NMR spectrum of C_{70} consists of five peaks: It is consistent with the concept of the structure of C_{70} , which is obtained from C_{60} by introducing a band of 10 carbon atoms in the equatorial region of the sphere and subsequent extension of the cluster.

The C_{70} molecule structure was analyzed numerically on the basis of measurements of the electron energy loss spectrum for electron collisions with the C_{70} molecule in

TABLE I. Properties of different kinds of C–C bonds in the C_{70} molecule.³⁶

Bond	Number of bonds of this type	Type of bond	Bond length, nm
1	5	hexagon-hexagon	$0.141^{+0.003}_{-0.001}$
2	20	hexagon-hexagon	0.139 ± 0.001
3	10	hexagon-pentagon	$0.147^{+0.001}_{-0.003}$
4	20	hexagon-pentagon	0.146 ± 0.001
5	10	hexagon-hexagon	0.137 ± 0.001
6	20	hexagon-pentagon	0.147 ± 0.001
7	10	hexagon-hexagon	0.137 ± 0.001
8	10	hexagon-pentagon	0.1464 ± 0.0009

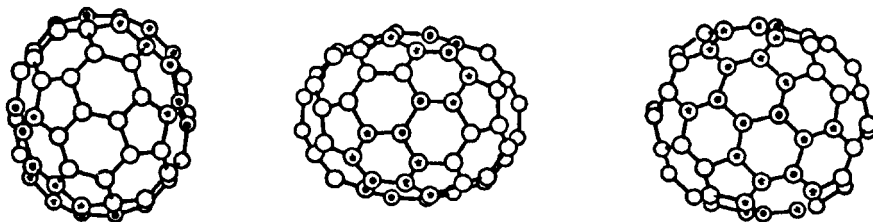


FIG. 7. Structure of the C_{76} molecule. The filled and unfilled circles and the circles with asterisks correspond to the different locations of atoms in the structure.³⁷

the gaseous state.³⁶ The spectrum gives as many as 8 different types of C-C bonds whose notations are given in Fig. 6 as they were introduced in Ref. 36. Table I lists some parameters of these bonds. As it is seen, the lengths of bonds 3, 4, 6, 8 are close to 0.146 nm. A bond of these types borders with a pentagon and hexagon, and connects two hexagons. The lengths of bonds 5, 7 that border with hexagons and connect two pentagons are equal to 0.137 nm. The bonds 1, 2 located on the boundary of two hexagons have intermediate values of the length.

Compare the lengths of bonds for the C_{70} molecule with those of graphite and the C_{60} -molecule. One can see that a bond of type 1, which is not deformed by the proximity of a pentagon, is similar to the C-C bond in a layer of graphite. The length of this bond ($0.141^{+0.003}_{-0.001}$ nm) is essentially the same as the corresponding value for graphite (0.142 nm). The lengths of bonds located on the boundary of two hexagons and connected a pentagon and hexagon are equal to 0.144 and 0.146 nm for C_{60} and C_{70} correspondingly, and the lengths of bonds-sides of a pentagon and hexagon are equal to 0.139 and 0.137 nm. The total length of the C_{70} molecule, determined as the distance between the pentagonal faces situated in two opposite polar regions, is equal to 0.780 ± 0.001 nm.³⁶ The diameter of the equator circle which passes through centers of carbon atoms is 0.694 ± 0.005 nm.³⁶ It is of interest that the diameter of the following circle which passes through carbon atoms of the neighboring layers is equal 0.699 ± 0.005 nm according to Ref. 36. Authors conclude that there is a waist in the equatorial region of C_{70} . But the accuracy of the above

measurements is not enough for the reliable conclusions concerned to fine details of the form of the cluster C_{70} .

Note that fullerenes under consideration C_{60} , C_{70} , C_{76} , C_{84} consist of 12 pentagons and 20, 25, 28 and 32 hexagons correspondingly. The more is the fullerene size, the less is its symmetry. The NMR spectrum of C_{76} includes 19 resonance peaks of approximately similar intensity.³⁷ It means that carbon atoms in the C_{76} molecule can occupy 19 different locations, where each of the 19 groups consists of four atoms. The surface of C_{76} is composed of 12 pentagons and 28 hexagons. The structure of this molecule can be reproduced from C_{60} if two C_{60} "polar caps," each consisting of a pentagon surrounded by hexagons, are encircled alternately by pentagons and hexagons, after which the two are joined, with the pentagons being kept away from each other by means of the hexagons. A closed structure is obtained by adding an additional pair of pentagons and a pair of hexagons. Figure 7 displays the structure of C_{76} , oriented perpendicular to each of the three symmetry axes of the molecule.³⁷ The lengths of three main axes of the ellipsoid C_{76} are equal correspondingly to 0.879, 0.764, and 0.668 nm.

Additional information about the fullerene structures follows from studies of charged clusters C_n^+ . Fig. 8 contains the data about mobilities of charged clusters C_n^+ moving in gases under the action of electric field.³⁸ As it is seen, several values of the mobility correspond to the same n . It means that there are different isomers of C_n^+ which can be formed in gases. Each of the set of curves corresponds to the certain structure of charged clusters. For example,

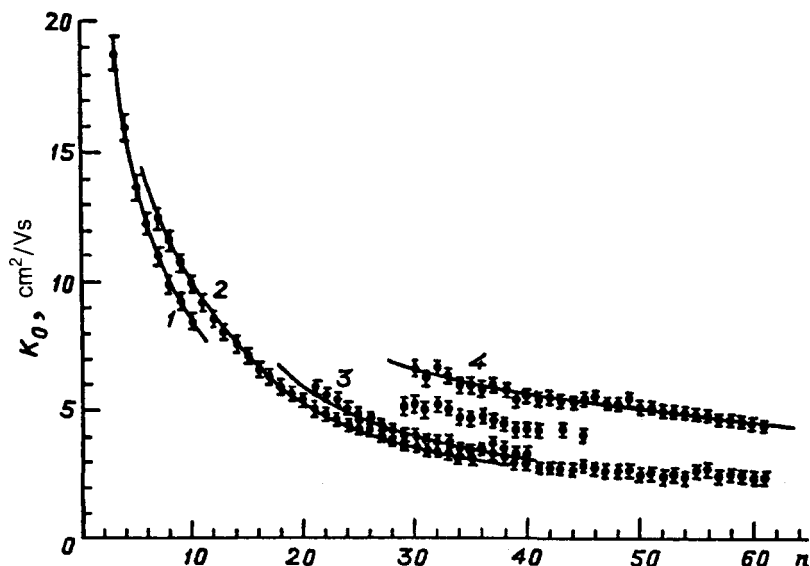


FIG. 8. Mobility of C_n^+ clusters in helium as a function of their size n (Ref. 38). The reduced values of the mobility relate to standard conditions.

dark points of Fig. 8 (curve 1) correspond to linear clusters existing for $n=3-12$. The curve 2 relates to clusters with the planar cyclic structure³⁸ formed with $n=6-36$. Curve 3 with $n=21-61$ respects to other cyclic structure which according to the conclusion³⁸ consists of two cyclic fragments. It is natural to expect that the mobility of the C_n^+ isomer having a closed cyclic structure is greater than that of an isomer with a linear structure containing the same number of atoms. Trace 3, which connects clusters with $21 \leq n < 61$, is quite close to curve 2, so von Helden *et al.*³⁸ ascribed it to a planar closed cluster structure containing two closed cyclic formations. Curve 4, which connects clusters with $30 \leq n < 61$, was ascribed to fullerenes and clusters with three-dimensional closed structures. This is inferred from the mobility, which is greater than that of clusters of the same mass having planar structure. Evidence for this also comes from comparing the mobility of the C_{60}^+ cluster shown on curve 4 of Fig. 8 with the value obtained by measuring the mobility of a positively charged C_{60}^+ cluster introduced into the drift chamber from outside. The points located between curves 3 and 4 relate provisionally to a three-cycle planar C_n^+ structure.

Fullerenes open a new class of molecules whose atoms are situated on a closed surface. The surface of fullerenes resulting from joining of nearest atoms consists of pentagons and hexagons, and according to the Euler's theorem it requires 12 pentagons and various numbers of hexagons to obtain a closed surface. Let us discuss the simplest of these structures, in which there are no hexagons. The surface of this C_{20} cluster consists of 12 pentagons, all vertices of which are located on a sphere.

This structure can be constructed in a simple way, as follows. Let us locate 20 atoms in 4 pentagons whose planes are parallel and whose vertices are located on the surface of a sphere. The sides of the uppermost and lowermost pentagons are equal to a , the distance between nearest neighbors of the figure; the sides of the other two pentagons are equal to $2a \sin(\pi/5) = 1.618a$. Since all the vertices of the pentagons are placed on the sphere, this means that the distance from the center to the planes of the large pentagons is equal to $0.263a$ and the distance to the planes of the small pentagons is equal to $1.174a$. Accordingly the radii of the circles made by crossing through the sphere along the planes in which the pentagons are located are equal to $0.851a$ and $1.376a$. The radius of the sphere in which the vertices of the pentagons are located is equal to $1.401a$.

As was noted, if we join the nearest vertices of pentagons lying on the surface of a sphere we obtain the surface of a figure consisting of 20 regular pentagons. This structure is symmetric with respect to a rotation through an angle equal to a multiple of $2\pi/5$ about the axis perpendicular to the planes of the large and small pentagons. One can choose any axis which passes through the sphere center and is perpendicular to a surface of pentagons as the symmetry axis. Thus, this cluster has a high symmetry. There are 6 different axes of symmetry and 24 transformations which lead to changing of positions of individual at-

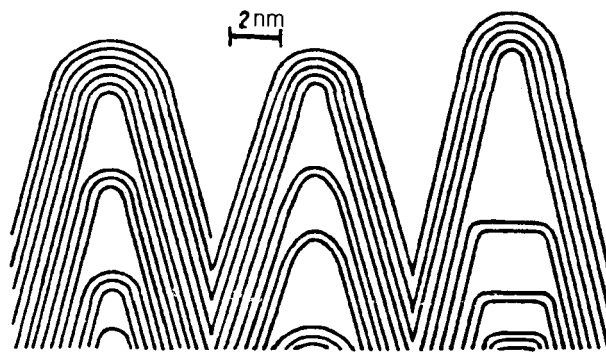


FIG. 9. Photograph of the cross section of the free end of a microtubule, taken using an electron microscope.¹²⁷ Each line corresponds to a distinct layer consisting of hexagons (on the straight portion) or hexagons and pentagons (in the curved portion). The separation between neighboring layers is 0.34 nm.

oms with conservation of the structure under consideration.

Because of a high symmetry, the binding energy of carbon atoms in molecule C_{20} is higher than in clusters with near numbers of carbon atoms. Therefore, the molecule C_{20} is more stable in comparison with nearest molecules and structures. But it does not mean the possibility to assemble such a molecule. Indeed, in the case of the assembly of a C_{60} molecule from graphite we already had individual elements of the molecule. They could be obtained by breaking a graphite surface into separate fragments consisting of hexagons, which could then be joined into the molecules. Since the C_{20} molecule contains no hexagons, it must be assembled from individual atoms, which makes the actual creation of a C_{20} molecule problematical. Nevertheless, Castleman and his collaborators at the University of Pennsylvania¹⁴⁹ have obtained Ti_8C_{12} molecules, which are analogs of C_{20} , since they have the same structure.

As we discussed above, in fullerenes each atom has three nearest neighbors. In the Ti_8C_{12} molecule each titanium atom has three carbon atoms as neighbors, and each carbon atom has two titanium and one carbon atom. All of the carbon atoms, and also all of the titanium atoms, are equivalent, which implies that the Ti_8C_{12} molecule has high symmetry and, correspondingly, a high stability. The high rate at which these molecules form when organic molecules interact with titanium¹⁴⁹ opens up a new class of compounds, molecules which have fullerene structure, i.e., all atoms of these compounds are located on a closed surface.

In the process of producing fullerenes from graphite various intermediate structures also form, based like graphite on a ring of six carbon atoms. The limiting case of these structures, which has been studied in detail in Refs. 124-127, is that of fullerenes with extended structure. These structures are called microtubules.

Fig. 9 contains the examples of microtubules. They are formed in an arc discharge with carbon electrodes. The temperature of a zone of their production is near 3000 K.

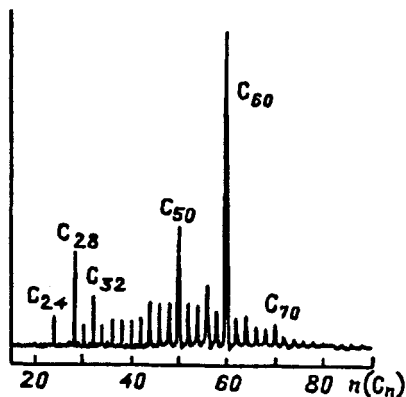


FIG. 10. Typical mass spectrum of the products of thermal vaporization of graphite.¹³

The electronic microscope photography shows a layer structure of microtubules with the distance between nearest layers 0.34 nm (as in graphite). The length of microtubules is of the order of microns. Evidently, microtubules are produced in some region of discharge where the gas temperature is in a certain interval. Then one can explain the large length of these structures. Usually, one end of a microtubule is connected to the surface, while the other remains free.

Such objects evidently have the same structures as fullerenes. Indeed, their basis is individual graphite fragments consisting of some set of hexagons. To join the hexagonal fragments into a three-dimensional closed structure it is necessary to have a certain number of pentagons, which are responsible for the curving of the hexagonal network in space and which convert this network from planar into three-dimensional. The existence of carbon microtubules reflects the variety of forms of carbon that occur in high-temperature nonequilibrium processes. Probably, these are among the constituents of carbon soot. The discovery of microtubules opens a new field of studies related to research of fullerenes.

2.3. Generation of fullerenes

Since the structure of fullerenes is close to that of graphite, the most effective approach to synthesizing them is based on thermal evaporation of graphite. A typical mass spectrum of the charged carbon clusters resulting from laser vaporization of graphite is shown in Fig. 10 (Ref. 13). As can be seen, the clusters with an even number of carbon atoms are the most stable ones.

In selecting the optimum conditions for producing C_{60} clusters it is necessary to take into account the fact that the graphite must not be overheated. This ensures that the bonds between neighboring graphite layers are destroyed, but does not break the vaporized carbon down into individual atoms. Then the vaporized graphite will consist of fragments containing hexagonal configurations of carbon atoms. It is from these fragments that the C_{60} clusters are assembled.

The vaporization of graphite, which is accompanied by the formation of a flux of these fragments from its surface, takes place either as a result of ohmic heating of a graphite electrode,¹⁸ or through laser irradiation of the graphite surface.¹⁵ Here an important role is played by the buffer gas, which is usually helium. The fundamental role of helium is probably associated with cooling of the fragments; by taking away their vibrational energy released as a result of fragments joining. Because of a small mass, helium atoms fulfill a role of quenching atomic particles better than other atoms or molecules. An experience shows that the optimum helium pressure for fullerene generation is in the range of 50–100 Torr.

As can be seen from Fig. 10, the stream of fragments formed as a result of thermal vaporization of a graphite surface contains in addition to C_{60} and C_{70} clusters a large number of lighter clusters with an even number of carbon atoms. Under the corresponding conditions a considerable fraction of these clusters is converted into C_{60} and C_{70} clusters. For this it is necessary to keep carbon deposit formed as a result of thermal vaporization of graphite over a period of several hours either at a temperature of 500–600 °C, or at a lower temperature in a nonpolar solvent. Though the kinetics of C_{60} and C_{70} production under these conditions is not known in detail, but it includes some processes of formation and breaking of carbon bonds. As a result of such processes clusters with enhanced stability form. Thus, when a fairly long time has passed, the largest portion of the carbon deposit is converted into the stable forms C_{60} and C_{70} . Thus, the procedure for production of a carbon deposit with a high fullerene content consists of two stages. The first stage consists of thermal vaporization over sputtering of the graphite surface, and the second

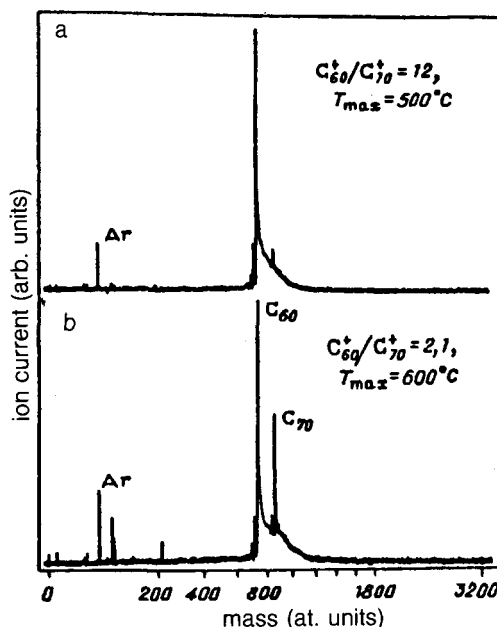


FIG. 11. Mass spectrum of clusters resulting from vaporization of the carbon deposit formed by laser irradiation of graphite,¹⁴ the temperature of the vaporizing cell was 500 °C (a) and 600 °C (b).

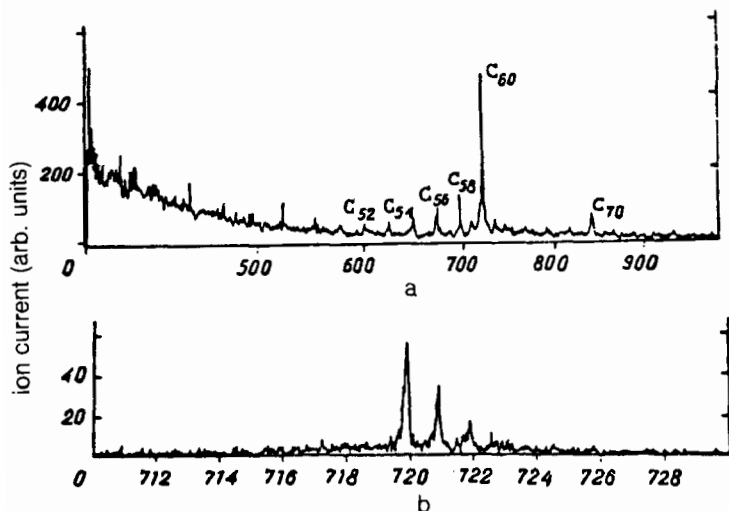


FIG. 12. Mass spectrum of carbon cluster ions formed through vaporization of graphite electrodes in a helium atmosphere.¹⁷ a) Low-resolution spectrum; b) high-resolution spectrum, where the peaks $M=721$ and 722 correspond to C_{60} clusters with one and two ^{13}C isotopes.

involves combining the products of this sputtering into a stable compound. These considerations determine the complexity of the technique for producing a carbon deposit with a high relative content of C_{60} .

Let us analyze the fullerene production procedures in detail. In Refs. 15–17 a carbon deposit was produced by electric heating of a graphite electrode (the graphite purity was 99.99%) in helium at a pressure of 100 torr and was collected on a glass disk. Approximately 20 mg of the black powder obtained this way, which was scraped from the disk in air, was packed into a small crucible made of stainless steel and having a nozzle with an internal diameter of 2 mm. The crucible was placed in a chamber in which the pressure was maintained at 10^{-5} torr. The crucible was heated to a temperature of 500–600 °C, causing particles of the carbon deposit to flow out through the nozzle. These were then collected on a thin tungsten ribbon, creating a layer of several microns thickness there. The carbon deposit was analyzed by means of its vaporization with a KrF laser having a pulsed energy of 60 mJ and beam diameter of 0.25 mm, and the mass spectrum of forming particles was studied. Laser irradiation of a tungsten ribbon with a deposited layer of carbon deposit causes it to be desorbed from the surface. The forming particles were ionized using an ArF laser with a pulsed energy of 200 μ J and a beam diameter of 1.5 mm. Figure 11 shows mass spectra of the carbon deposit obtained in this manner at two values of the temperature of the evaporation crucible. As can be seen, in both cases the C_{60} cluster dominates; the C_{70} cluster also makes a noticeable contribution. The signals produced by the presence of C_{58} , C_{56} , and C_{54} clusters are barely detectable. Argon was used as a buffer gas in the measurements.

A somewhat more elaborate technique for preparing a carbon deposit with a high C_{60} content was used in Refs. 17–19. In this technique also the initial stage involved the ohmic heating process and thermal vaporization of a graphite electrode in a helium atmosphere at a pressure of 100 torr. The carbon deposit thus formed was carefully scraped from the collector surface and dissolved in benzene. After this is evaporated a dark brown or black crystalline substance precipitates from the suspension. Other

nonpolar solvents such as toluene, CS_2 , CCl_4 have been used successfully instead of benzene. The measurements show that using a suspension significantly increases the relative yield of the C_{60} clusters. This technique allows up to 100 mg of carbon deposit with a high C_{60} content to be prepared per day with a single device. Typical mass spectra of the product, obtained using a time-of-flight mass spectrometer, are shown in Fig. 12. This deposit was vaporized by irradiating it with a beam of Ar^+ ions of energy 5 keV. The ratio of the yield of C_{70}^+ ions to that of C_{60}^+ was equal to ~ 0.1 . Using an electron beam instead of Ar^+ ions resulted in a decrease in this ratio to ~ 0.02 . Ratios of this order were obtained with laser radiation of the carbon deposit.^{8,39} The subsequent development of this technology⁴⁰ is based on a chromatographic separation of clusters C_{60} and C_{70} .

The technology of the fullerenes production with the use of dissolving of the carbon deposit^{17,18} provides the C_{60} output at rates on the order of a gram per hour.^{41,42} The design of this apparatus is shown in Fig. 13. It is based on a pair of graphite electrodes, one of which is a flat disk and the other is a pointed rod of diameter 6 mm pressed against the disk by means of a soft spring. The electrodes together with measurement apparatus are placed in a water-cooled copper chamber in the shape of a cylinder of diameter 8 cm and length 15 cm. The chamber is filled with helium at a

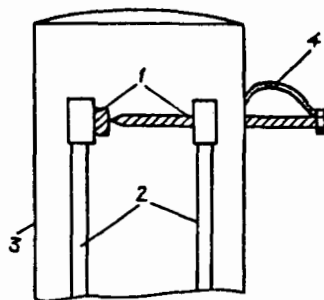


FIG. 13. Schematic of the device used to produce C_{60} in gram quantities.⁴¹ 1) Graphite electrodes; 2) water-cooled copper ribbon; 3) water-cooled surface for collection of the carbon deposit; 4) springs.

pressure of ~ 100 torr. The graphite is vaporized by passing an alternating current with frequency 60 Hz and carrying 100–200 A at a potential of 10–20 V through the electrodes. The compression of the spring was controlled so that the electric arc burns between the disk and rod electrodes, and the main part of the input power releases in the arc. This regime also provides the vaporization rate ~ 10 g/h. As a result of arc heating over several hours the surface of the water-cooled copper chamber became covered with graphite soot, which was carefully scraped off the surface and exposed to boiling toluene for approximately 3 h. The resulting dark brown liquid was vaporized in a rotating evaporator, which resulted in the formation of a dark powder whose weight was $\sim 10\%$ of the initial graphite soot. Spectral analysis reveals that this powder consists of clusters C_{60} and C_{70} in a ratio of approximately 10:1. Thus, this technique allows C_{60} to be obtained in quantities sufficient for carrying out laboratory studies.

Some modernization of this technology can change the output parameters. For example, in Ref. 43 the main features were used of the above setup and somewhat different parameters of the process. In contrast to the work of Haufier *et al.*⁴¹ cited above, in Ref. 43 two sharply pointed graphite electrodes were used with the points juxtaposed, and worked at somewhat lower energy inputs (potential 5–8 V, current 100–180 A, frequency 60 Hz) and helium at higher pressures (180 torr). Besides, toluene was used as a solvent. The yield of this device was about 50 mg/h of pure C_{60} . The high purity of the C_{60} thus obtained was confirmed by both mass-spectrometric and nuclear magnetic resonance measurements.

For purification and enrichment of the product the methods of liquid chromatography⁴⁰ are used. It allows both to divide C_{60} from C_{70} , and to extract other fullerenes as C_{76} , C_{84} , C_{90} , C_{94} (Ref. 44). About 500 mg of carbon deposit formed through thermal evaporation of a graphite electrode during the burning of an electrical arc was adsorbed by the surface of an aluminum plate of mass 250 g. Processing this surface with a mixture of hexane and toluene in the ratio 95:5 led to fractionation and subsequent separation of pure C_{60} . Pure C_{70} could be separated by increasing the toluene content in the solution to 50%. Further gradual increase in the toluene content in the solution allowed four yellowish fractions to be separated, which were subjected to repeated chromatographization on the aluminum surface. As a result they were able to separate the fullerenes C_{76} , C_{84} , C_{90} , and C_{94} in essentially pure form. Thus, processing the first of these fractions absorbed on the aluminum surface with a mixture of hexane and toluene in the ratio 95:5 resulted in complete dissolution of the C_{70} clusters in the mixture. The remainder of the yellowish deposit consisted almost entirely of C_{76} clusters which confirmed the results of the liquid-chromatographic analysis. These results are exhibited in Fig. 14, which shows the profiles of the high-pressure liquid chromatography obtained by using chromatographic columns with dimensions 24×0.5 cm² and *n*-hexane as a solvent. Parameters of the process are: a pressure of 100 atm, and the rate of dissolvent 2 ml/min. The fullerenes C_{76} , C_{84} , C_{90} , and

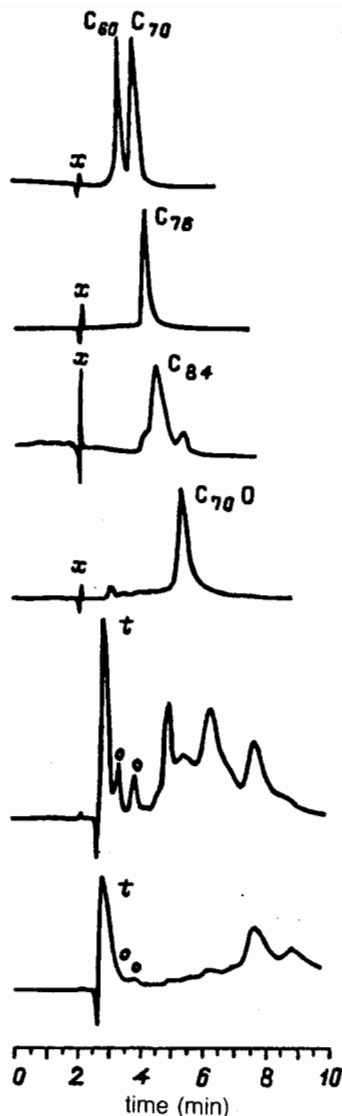


FIG. 14. High-pressure liquid-chromatographic profiles of the components extracted from the carbon deposit.⁴⁴

C_{94} were identified with a time-of-flight mass spectrometer. Along with these molecules the mass spectra revealed the cluster $C_{70}O$, which formed due to the presence of traces of oxygen in the working volume. It follows from the results of the chromatographic and mass-spectrometric analysis that the fraction by weight of the higher fullerenes C_{76} , C_{84} , C_{90} , and C_{94} in the original carbon condensate, which consisted mostly of C_{60} and C_{70} clusters, was 3–4%. Thus, this technique allows one to obtain fullerite, material consisting essentially of fullerenes of a specified type, in milligram quantities. An improvement of this chromatographic technique as distillation of fullerene deposit at boiling of the dissolvent^{132,133} allows both to increase the output of the technology and to improve the product purity.

It is of interest to note that graphite is not the only material that can be used effectively to obtain C_{60} . A good example is the use of the liquid-crystal tar as a source or C_{60} (Ref. 45); this is formed by pyrolysis of some organic

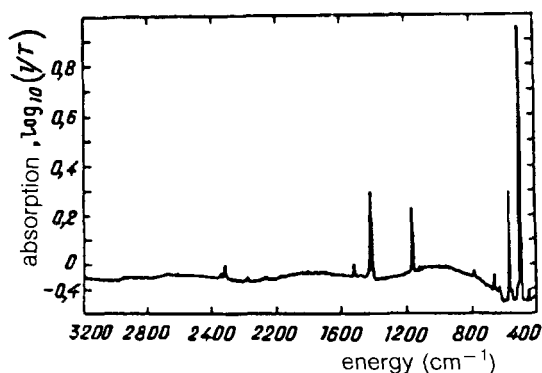


FIG. 15. The infrared absorption spectrum of a layer of C_{60} clusters of thickness $\sim 2 \mu\text{m}$ deposited on a transparent silicon substrate.^{17,18} Here T is the fraction of the radiation which passes through the substrate. The appearance of a negative absorption is due to reflection of the radiation by the substrate.

compounds at temperatures 370–500 °C (Ref. 46). The liquid-crystal mesophase used in the work of Dance *et al.*⁴⁵ was a tarry substance formed by continuous hydrogenation of coal lignite at a hydrogen pressure ~ 100 atm for 2.5 h. After removal of the volatile fragments at $T=400$ °C in a chamber maintained at reduced pressure a tar formed, characterized by an aromaticity of 0.82 and consisting of 92.7% C, 4.8% H, 1% N, and 1.5% O. Laser irradiation of such a tar leads to formation of a light fraction consisted of 60–100% fullerenes C_{60} .⁴⁵ According to mass-spectral studies the C_{60} fullerene output of this method depends on the kind of buffer gas used. The variety of compounds which can be used for production of the initial tar allows us to choose the optimal methods for production of C_{60} from hydrocarbons. Reviews of recent achievements in the industrial production of fullerenes are found in Cox *et al.*¹³⁴ and Malhotra.¹³⁵

2.4. Spectroscopy of fullerenes

Spectral studies of fullerenes give a reliable way for both fullerene detection and analysis of their structure. For example, a poor infrared spectrum of C_{60} proves a high symmetry of this fullerene and determines its structure.^{18,47} Typical infrared and visible absorption spectra from carbon deposit coated in a thin layer on a transparent quartz plate are shown in Figs. 15 and 16 (Refs. 17 and 18). Four strong absorption lines 1429, 1183, 577, and 528 cm^{-1} with the width varying over the range 3–10 cm^{-1} stand out in the spectrum. In samples prepared using the isotope ^{13}C with a purity of 99%, the absorption lines are shifted toward the red part of the spectrum. The above values of the absorption frequencies agree approximately with the results of calculations^{48–52} performed under the assumption that the structure of C_{60} is that of a truncated icosahedron.

A high symmetry of the cluster C_{60} makes its absorption spectrum to be poor and its Raman spectrum to be rich. Fig. 17 contains some fragments of Raman spectrum for C_{60} .¹⁴ In these measurements carbon soot was deposited on a tungsten foil and was irradiated with argon laser

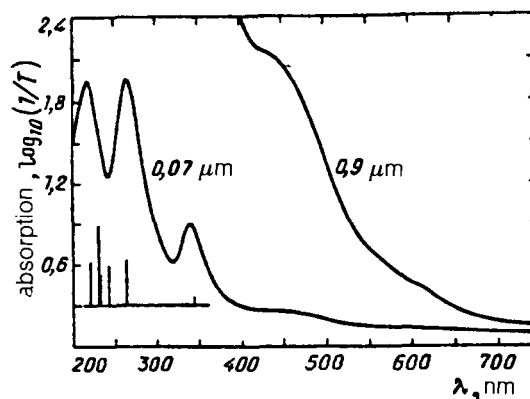


FIG. 16. The visible and ultraviolet absorption spectra of sputtered layers of C_{60} clusters of various thicknesses, deposited on a transparent quartz substrate.^{17,18} The diagram displays also the results of calculating the relative location and relative strengths of the oscillators for the allowed transitions of the C_{60} cluster.⁴⁸

radiation of the wave length $\lambda=514$ nm and of the power 1.4×10^{-5} W. The spectral resolution of used setup was 9 cm^{-1} . Note that fullerenes under consideration were prepared using the technique described in the previous section,¹⁴ and exhibit the mass spectra shown in Fig. 11a and b respectively. The difference in the spectra shown in Fig. 17a, b is explained by different content of C_{70} in the analyzed samples. Lines with frequencies 1568, 1232, 1185, 1062, and 260 cm^{-1} observed in the spectrum of Fig. 17b with a higher relative C_{70} content are ascribed to this clus-

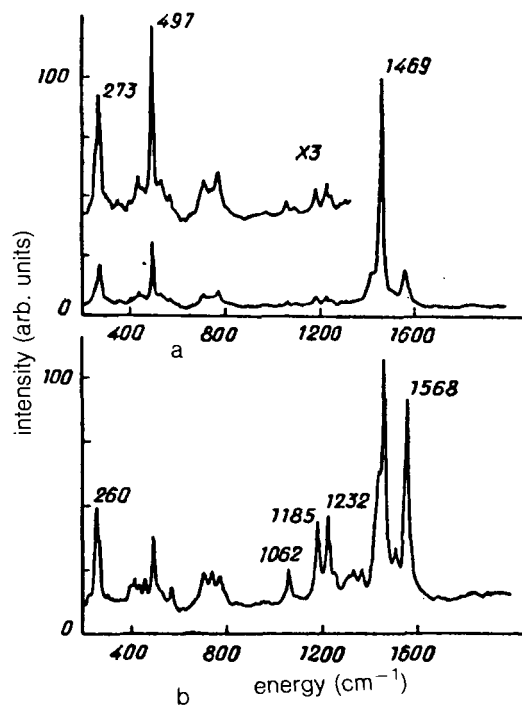


FIG. 17. Raman spectra of carbon deposit coated onto a tungsten foil.¹⁴ The temperature of the vaporization cell was $T_c=500$ °C (a), 600 °C (b).

TABLE II. Raman frequencies, relative intensities, and depolarization coefficients for the Raman scattering lines of fullerene-bearing carbon powder.¹⁴ The values of I_a and I_b correspond to the conditions of Fig. 11a, b.

ν, cm^{-1}	I_a	I_b	$\rho(\pm 0,02)$	Identification
260	7	34		C_{70}
273	17	17		$\text{C}_{60}, \text{H}_g$
413		9		
435	5	6		
457		9		$\text{C}_{60}, \text{A}_g$
497	27	27	0,16	
571	2	9		
705		13		
711	4			
739		13		
773	6	13		
1062	2	14	0,23	C_{70}
1185	4	34	0,19	C_{70}
1232	4	36	0,19	C_{70}
1336		11		
1370		11		
1430	13			
1448		32		
1469	100	100	0,11	$\text{C}_{60}, \text{A}_g$
1513	3	15		
1568	15	88	0,24	C_{70}

ter. Lines with frequencies 1469, 497, and 172 cm^{-1} observed in these spectra are ascribed to the C_{60} cluster.

Table II displays the frequencies, relative intensities, and identification of the Raman scattering lines of carbon deposit shown in Fig. 17. For the strongest lines the depolarization parameter $\rho = I_{\perp} / I_{\parallel}$ is given, where I_{\perp} and I_{\parallel} are the intensities of the scattered radiation corresponding to the combination frequency with polarization perpendicular and parallel to that of the incident radiation. The high polarization of the scattered radiation, which characterizes the two strongest C_{60} lines (497 and 1469 cm^{-1}) indicates that these lines are related to the completely symmetric vibrational modes of this molecule. Note the close coincidence of the experimental Raman frequency [14] $\nu = 273 \text{ cm}^{-1}$ with the theoretical calculations^{17-19,30,31} fulfilled before experiments. According to these calculations, the vibration frequency of a truncated icosahedron corresponding to the transformation of the sphere into an ellipsoid (the "squashing" mode) is equal to $273 \pm 10 \text{ cm}^{-1}$ (Refs. 17-19, 30, 31), where the indicated error is the result of a statistical average of the data from these different authors. The values of the frequencies 1469 and 497 cm^{-1} , attributed to the completely symmetric oscillation modes are in somewhat poorer agreement with the calculations. The calculated values of these frequencies, of which the first corresponds to stretching and compression of the pentagonal faces of the icosahedron and the second to the "breathing" modes, lies in the range 1627-1830 and 510-660 cm^{-1} .

The most complete information about the vibrational spectra of the C_{60} molecule was obtained from experiments on inelastic scattering of slow neutrons.⁵³⁻⁵⁵ This is related to the fact that inelastic scattering of a slow neutron by a molecule can efficiently excite all molecular oscillation modes, regardless of their symmetry. As shown by group-

TABLE III. Comparison of the vibrational frequencies of C_{60} molecules measured by inelastic neutron scattering, optical absorption, and Raman scattering (see Ref. 54).

Identification	Frequency, cm^{-1}		
	Neutron scattering	Optical absorption	Raman scattering
Lattice vibrations	96,6	—	—
	145	—	—
	234	—	—
H_g	266	—	273
$\text{T}_{2u}, \text{G}_u$	346,354	—	—
H_u	403	—	—
H_g	443	—	437
G_g, A_g	483	—	496
T_{1u}	531	523	—
T_{1u}	572	572	—
	620	—	—
	669	—	—
H_g	708	—	710
	740	—	—
H_g	773	—	774
	837	—	—
	877	—	—
	919	—	—
	960	—	—
	1000	—	—
	1060	—	—
H_g	1100	—	1100
	1120	—	—
T_{1u}	1180	1180	—
	1200	—	—
H_g	1260	—	1250
	1350	—	—
$\text{H}_g, \text{T}_{1u}$	1420	1430	1430
A_g	1480	—	1470
H_g	1580	—	1570

theoretical analysis,⁵⁶ of the 174 possible types of oscillation in a C_{60} molecule it is possible to distinguish 46 fundamental modes, of which two are characterized by A_g symmetry, one by A_u , three by T_{1g} , four by T_{1u} , five by T_{2u} , six by G_g , six by G_u , eight by H_g , and seven by H_u . Four of these oscillation modes, characterized by T_{1u} symmetry, are active in the optical absorption spectra; ten (H_g, A_g) are active in the Raman scattering spectra; and the others cannot be detected optically.

In Table III are shown values of the frequencies corresponding to the peaks in the neutron energy loss spectra resulting from scattering by C_{60} molecules at $T = 20 \text{ K}$ (Ref. 54). These values, which have been identified in connection with the symmetry of the molecular oscillations, are compared using the results of measurements made by optical absorption and Raman scattering techniques. As can be seen, the most complete information about the vibrational spectrum of the molecule is contained in the inelastic neutron scattering data. The unidentified neutron energy loss peaks are probably related to excitation of combined oscillations. Some discrepancies in the values of the energy corresponding to the optical absorption peaks and the neutron energy loss peaks are due to poor resolution for resonances of neutron scattering. Note also that some types

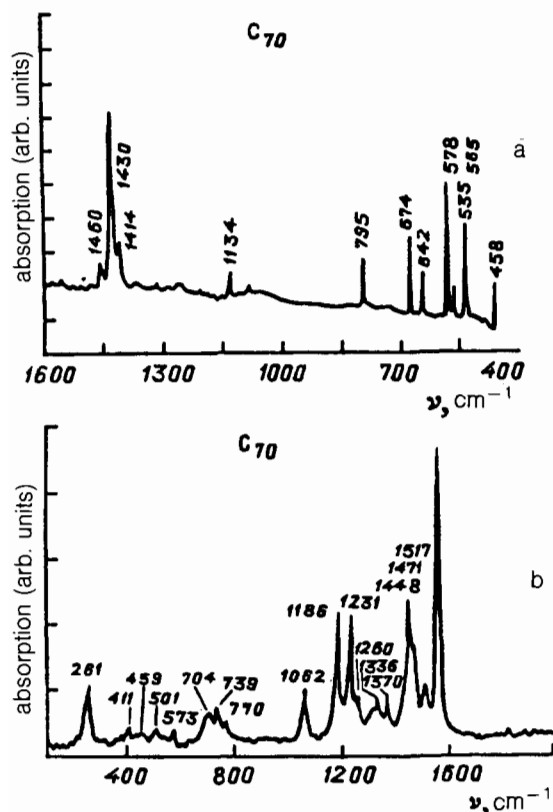


FIG. 18. Spectral characteristics of C_{70} -clusters coated onto substrate.⁵⁷ (a) The infrared absorption spectrum with KBr substrate. (b) Raman spectrum for nonpolarized radiation and suprasil as a substrate.

of oscillation observed in Refs. 54 and 55 are attributed there to different types of symmetry.

The development of the liquid chromatography methods for extraction of different fullerenes and production of pure fullerenes gave a possibility to study the properties of higher fullerenes. As a demonstration of it in Fig. 18 are depicted the Raman spectra for the molecule C_{70} .⁵⁷ As it is seen, the molecule C_{70} has more active vibrations than C_{60} because of its lower symmetry. Fig. 19 contains the absorption optical spectra of the molecules C_{70} , C_{76} and $C_{76}O$ dissolved in n -hexane.^{44,58} According to measurements the molecule C_{76} has several absorption bands with centers at $\lambda = 230, 286, 328, 350, 378, 405, 455, 528, 564, 574, 709$ and 768 nm. The absorption spectrum of the molecule C_{84} consists of several bands with centers at $\lambda = 280, 320, 380, 303, 476, 566, 616, 668, 760$ and 912 nm. Fig. 20 contains the infrared spectra of absorption for the molecule C_{76} .³⁷ Detailed studies of the spectra permit absorption bands of C_{76} with centers at $\lambda = 230, 286, 328, 350, 378, 405, 455, 528, 564, 574, 642, 709$ and 768 nm to be resolved. The absorption spectrum of C_{84} contains bands with centers at $\lambda = 280, 320, 30, 393, 476, 566, 616, 668, 760$ and 912 nm. The infrared absorption spectra of C_{76} are shown in Fig. 20 (Ref. 37).

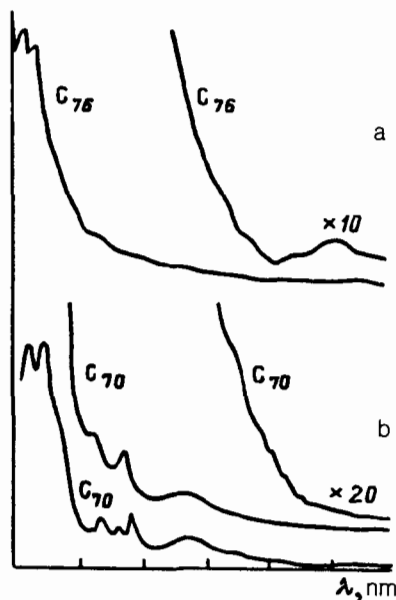


FIG. 19. Optical absorption spectra of the higher fullerenes dissolved in n -hexane: C_{76} (Ref. 44) (a), $C_{70}O$ (Ref. 44) (b), and C_{70} (Ref. 58) (c).

3. FULLERENES IN GAS-PHASE SYSTEMS

3.1. Processes involving fullerenes

The results of studying the processes in which C_{60} and the other fullerenes participate imply that these carbon compounds have an anomalously high stability. The first experiments had already led to the same conclusion; in these the C_{60} cluster manifested itself among the other clusters as the one with a magic number of atoms. Study of monomolecular decay of carbon clusters with $n \geq 30$ reveals that the stability of clusters with an even number n is considerably greater than that of clusters with odd n . Both in the case of monomolecular decay¹² and in the case of

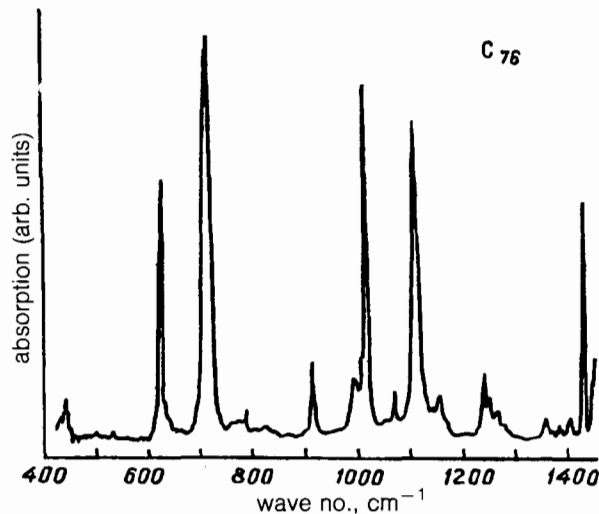


FIG. 20. The infrared absorption spectrum of C_{76} dissolved in CS_2 (Ref. 37).

TABLE IV. Parameters characterizing monomolecular decay of C_n^+ clusters by $C_n^+ \rightarrow C_{n-2} + C_2$ (Ref. 62).

n	$K_d, 10^4 s^{-1}$	$\langle E_t \rangle, eV$	Fraction of dissociated clusters	E_0, eV	E_{int}, eV
58	$1,7 \pm 0,5$	$0,4 \pm 0,1$	$0,19 \pm 0,02$	$4,5 \pm 0,5$	39 ± 2
60	$0,7 \pm 0,2$	$0,4 \pm 0,1$	$0,10 \pm 0,02$	$4,6 \pm 0,5$	39 ± 2
62	$3,3 \pm 0,5$	$0,4 \pm 0,1$	$0,30 \pm 0,02$	$3,0 \pm 0,5$	26 ± 2

photodissociation⁵⁹ the main channel for the decay of C_n molecules with even values of n results from the splitting off of the fragment C_2 . In and of itself this fact is surprising, since the binding energy of the C_2 fragment is less than that of C_3 (Ref. 60). In the decay of C_n clusters (with n odd) the splitting off of a carbon atom is the most probable. This is why clusters with even values of n survive, while the fraction of clusters with odd n is less than 1% (Ref. 59). The available experimental data may imply that the structural feature of C_n clusters with large values of n is the absence of acute angles in the faces.^{12,61-63}

Radi *et al.*⁶² carried out a more complete study of this question, measuring the energy spectra of monomolecular decay products of the clusters C_{58} , C_{60} , C_{62} . These measurements enable one to estimate the energy required to remove a C_2 fragment from these clusters, and also the height of the energy barrier which tends to prevent decay. Cluster ions of carbon produced through laser irradiation of a graphite rod were accelerated in an electric field to an energy of 8 keV, mass-selected with a permanent magnet, and detected by means of a photomultiplier. Processing the energy spectra of the decay products thus obtained allowed the value of the rate constant K_d for monomolecular decay to be determined, together with the average value $\langle E_t \rangle$ of kinetic energy released through decay, the average value of the energy E_0 required to remove a C_2 fragment from the cluster, and the average value E_{int} of the cluster internal energy. All these data are shown in Table IV, which also gives the fraction of each type of decayed cluster. As can be seen, the value of the rate constant for decay of the C_{60} cluster is several times smaller than the values for clusters differing by two in the number of atoms.

Some idea of the decay mechanism for the C_{60} cluster, and consequently of its structure, can be gained from analyzing the results of measuring the spread in the energy with which the decay products expand (in the center-of-mass coordinate system). The results obtained from processing the experimental data⁶² have been compared with those obtained from calculations performed using a model of the structure of the C_{60} cluster. As can be seen from the comparison, the results of the calculation are rather insensitive to the assumptions about the cluster structure and are mainly determined by the values of the cluster internal energy E_{int} and detachment energy $\langle E_t \rangle$ of a C_2 fragment incorporated in the calculation. Radi *et al.*⁶² were thus able to determine the parameters shown in Table IV. In analyzing these values one is struck by the slight difference in the energy characteristics of the C_{60}^+ and C_{58}^+ clusters, which however differ markedly from the corresponding

values of the C_{62}^+ cluster. This peculiarity in the experimental data may serve as an indication of the slight structural differences in C_{60}^+ and C_{58}^+ clusters. The greater proportion of the C_{60}^+ cluster in coal dust can then be explained on the purely kinetic basis associated with the relatively high probability for the process by which heavier clusters that accompany the formation of the C_{60}^+ cluster are destroyed, and hence the low value of the probability for destroying the C_{60}^+ cluster. However, there may be another explanation for this relation between the energetic properties of the C_{58}^+ , C_{60}^+ , and C_{62}^+ clusters, associated with the manner in which these clusters are obtained under experimental conditions.⁶² The high temperature of the graphite rod irradiated by a high-intensity laser results in the formation of carbon clusters with anomalously high internal energy content. It is possible that the structure of these clusters differs from that of particles formed through gasdynamic cooling of the coal dust particles in a buffer gas atmosphere. Obviously, the question of the relation between the energetic and kinetic properties of ion clusters of carbon and their structural properties requires further investigation.

The study of the decay of fullerenes subjected to ultraviolet irradiation casts additional light on the nature of the stability of these compounds. In this area the recently published series of studies carried out by Wurz *et al.*^{64,65} is noteworthy; they obtained the mass spectrum of the neutral decay products of C_{60} clusters subjected to simultaneous irradiation by photons with $\lambda = 308$ and 118 nm. In these papers a fairly complicated experimental technique was used. It included three sources of laser radiation at different wavelengths. The radiation at the second harmonic of a Q-switched neodymium laser ($\lambda = 532$ nm) was used to vaporize C_{60} molecules sputtered onto a substrate of stainless steel. The radiation from a XeCl laser at $\lambda = 308$ nm was used to photodissociate C_{60} in the gaseous phase. Ionization of neutral fragments from the photodecay of C_{60} was carried out using radiation at $\lambda = 118$ nm, which was produced by tripling the frequency of the neodymium laser twice. Time-of-flight mass spectra of the neutral products of C_{60} photodecay reveal that the decay results from absorption by the molecule of a number (~ 10) of laser radiation photons with $\lambda = 308$ nm. The electron excitation energy resulting from absorption of a laser photon by the molecule is quickly converted into molecular vibrational energy, which is distributed statistically over a large number of molecular degrees of freedom. As shown by calculations carried out recently,⁶⁶ in order that the C_{60} molecule, which has a minimum dissociation energy ~ 4.6 eV, undergo decay over the time of flight in the mass spectrometer ($\sim 10^{-5}$ s), its internal energy must be greater than ~ 30 eV. This agrees with the result of the experiment, in which the larger carbon clusters with even numbers of atoms were detected along with C_2 fragments.

Evidence for the enhanced stability of fullerenes having closed symmetric structure comes from results of experiments in which pair collisions involving these molecules were studied. Thus, Ben-Amotz *et al.*⁶⁷ determined that among the large number of C_n^{z+} carbon clusters with $n = 60-124$, $z = 2, 3$, only the clusters C_{60}^{z+} , C_{70}^{z+} , and C_{84}^{z+} ,

retain their structure when undergoing charge exchange with C_7H_8 molecules. When these ions collide with Xe atoms at an energy of 392 eV, C_{60}^z+ ions form. An energy greater than or of order of 1 keV is required to destroy the latter through collisions.^{12,59,62,68}

The destruction of C_{60}^+ clusters in collisions with O_2 molecules with energies 7–8 keV was studied by Doyle and Ross.⁶⁹ In addition to smaller clusters, as a result of collisions multicharged clusters C_{60}^{z+} formed, where $z=2-4$. This implies that a C_{60}^+ cluster can undergo collisional ionization without fragmenting. This possibility also affords additional evidence of the anomalously high stability of fullerenes.

Christian *et al.*⁷⁰ studied the ion–molecular reaction of a C_{60} cluster and a C^+ ion in the range of collisional energies 2–78 eV, using an ion of the $^{13}C^+$ isotope to identify the reaction channels. The measurements revealed that at collision energies above 10 eV the principal reaction channel is associated with the formation of the long-lived complex C_{61}^+ , whose decay time is greater than 10^{-3} s. The subsequent decay of this complex can be accompanied by charge exchange, i.e., the escape of a neutral carbon atom. The charge exchange accompanied most likely by isotope exchange, as a result of which a carbon atom originally located in the C_{60} structure appears as the fragment.

Fullerenes were found to exhibit interesting behavior in collisions between these molecules and the surface of solids.⁷¹⁻⁷⁴ Thus, in the work of Beck *et al.*⁷¹ it was determined that collisions between charged C_{60}^{\pm} , C_{70}^{\pm} , and C_{84}^{\pm} fullerenes and a polished graphite or silicon surface at an energy varying over the range from 0 to 200 eV lead to the loss of a considerable fraction of the kinetic energy, but do not result in the destruction of the fullerenes. Bushman *et al.*⁷⁴ also arrived at similar results when the energy of the charged C_{60}^+ clusters interacting with a surface of polished graphite varied from 150 to 450 eV. It was established that the scattering angle of the ions corresponds to nearly specular reflection from the surface, although the kinetic energy of the scattered ions was equal to 10–20 eV, independent of the collision energy.

3.2. Fullerene chemistry

Based on their structure, fullerenes can be regarded as three-dimensional analogs of the aromatic compounds. This provides a reason for viewing the chemistry of fullerenes as one of the most promising direction for organic chemistry. An idea of the possible paths that may be taken in this direction comes from the experimental works published in recent years, a brief summary of which is given below. One of the sharpest and most interesting problems in fullerene chemistry is related to evaluating the possibility of inserting atoms of some other kind inside the cage of the spherical or spheroidal molecule and studying the physical and chemical properties of the resulting complex. This problem was posed as early as the first experimental work, which was aimed at obtaining and studying the C_{60} cluster,^{75,76} and which announced that atoms of La, Ni, Na, K, Rb, and Cs had been inserted inside the C_{60}^+ ion. However, the results of this work appear to be inconsistent

with the results of experiments carried out later by others,^{77,78} who showed that in $C_{60}M^+$ structures (where $M=La, Fe, Co, Ni, Cu, Rh$) formed as a result of collisions of atoms with fullerenes, the metal atoms are situated outside the fullerene cage. The results of experiments on inserting He atoms into the cage of charged fullerene C_{60}^z+ ($z=1, 2, 3$) appeared to be more definite.⁷⁹⁻⁸² Thus, according to one of the most recent papers devoted to this topic,⁸¹ when He atoms collide with C_{60}^+ ions at energies of 3–8 keV not only is the fullerene destroyed with the release of a C_{2n} fragment, but C_mHe^+ ($m=48-60$) clusters also form, in which the helium atom is enclosed inside the fullerene. Evidence for this comes, in particular, from the fact that the collisional dissociation of C_mHe^+ complexes is accompanied by the release of a C_2 radical, and not an He atom as might have been expected from its location outside the fullerene cage. Smalley¹³⁶ has recently carried out a detailed review of the problem of the mutual arrangement of a fullerene and an atom bound to it.

As noted above, fullerenes stand out by their high chemical inertia with respect to monomolecular decay. Thus, the C_{60} molecule retains its stability in an inert argon atmosphere up to temperatures ~ 1200 K (Ref. 83). However, in the presence of oxygen, particularly in the open air, oxidation of this form of carbon accompanied by the production of CO and CO_2 is observed even at much lower temperatures. The results of calorimetric measurements⁹⁴ show that the intense oxidation of C_{60} is observed even at temperatures of order 500 K. The process, which lasts several hours, leads to the formation of an amorphous structure in which there are 12 atoms of oxygen per each original C_{60} molecule. When this happens the C_{60} molecule essentially loses its shape completely. Experimental data show that the bond energy of an atom of oxygen and a C_{60} molecule is equal to about 90 kcal/mol, which is about twice the corresponding value for graphite.⁸⁵ Comparison of these numbers enables us to determine the energy needed to form a C_{60} molecule from a quantity of graphite with the same number of carbon atoms: $\Delta H \sim 540-600$ kcal/mol. This agrees in order of magnitude with the result of the theoretical estimate $\Delta H \sim 800$ kcal/mol (Ref. 86).

At room temperature the oxidation of C_{60} proceeds only in the presence of photons with energy in the range 20–1200 eV or 0.5–5 eV (Ref. 87). Kroll *et al.*⁸⁷ relate this fact to the necessity of forming the negative ions O_2^- , which possess an elevated reactivity at room temperature.

Since fullerene molecules have an electron affinity, in chemical processes they behave like weak oxidizers.⁸⁸ This property of fullerenes was apparent even in the first experiments on their chemical transformation,⁴¹ where hydrogenation of C_{60} was carried out. The result of hydrogenation turned out to be the $C_{60}H_{36}$ molecule. This result is quite surprising, since the structure of the C_{60} molecule includes 30 double bonds, each of which can combine with two hydrogen atoms. Based on this, one would expect the formation of the compound $C_{60}H_{60}$. Probably, one of the double bonds making up the regular pentagons in the C_{60} structure remains without a hydrogen atom. In accordance with the assumption of Haufler *et al.*,⁴¹ these bonds are

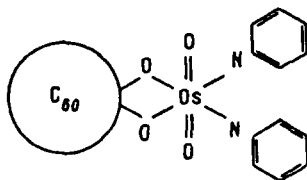


FIG. 21. Chemical structure of osmiated C_{60} (Ref. 91).

located on the surface of the sphere so that between each pair of double bonds there are two single bonds.

Even the earliest experiments on synthesizing organic compounds displayed an exceptionally broad variety of possibilities. Thus, in the work⁸² performed by the Wudl group as large as 12 compounds of C_{60} were synthesized and described. Among these compounds, which acquired the general designation "fulleroids," we can point out the products of combination with the radicals of hydrogen, phosphorus, the halogens, metals and their oxides, single and double benzene rings and their products, NO_2 (Ref. 88), and alkyl radicals.⁸⁹ Among specialists the work of Hawkins *et al.*⁹⁰ has aroused particular interest (see also the review in Ref. 91), where as a result of the reaction between C_{60} and OsO_4 a metallorganic compound $C_{60}(OsO_4)(4\text{-tert-butylpyridine})_2$ was obtained which exhibits ferromagnetism. The structure of this compound, established as the result of a series of elegant experiments, is shown in Fig. 21. Subsequent work by others confirmed the expectation⁹² regarding the wealth of promising developments in the field of fullerene metallorganic chemistry. The creation and study of such metallorganic complexes based on C_{60} as $[(C_6H_5)_3P]_2X(C_{60})$ (Ref. 93), $[(C_6H_5)_3P]_2(CO)ClX(C_{60})$ (Ref. 94), and $\{[(C_2H_5)_3P]_2X\}_6C_{60}$ (Ref. 93) have been announced, where the symbol X represents a metal of the platinum group Pt, Ir, Pd. The results of the experiments carried out by Fagan *et al.*⁹² show that adding a metallorganic radical to fullerene reduces the electron affinity of this molecule. This changes the electrical properties of fullerenes, opening the possibility of creating a new class of organic semiconductors with parameters varying over a wide range.

The first successful attempts to synthesize polymers on the basis of C_{60} also deserve close attention.⁸⁸ Here the C_{60} molecules play a double role: either as the building block for the polymer chain or as the connecting element. In the first case, for which the figurative name "thread of pearls" is used, connection of the fullerenes is accomplished by means of benzene rings. The second case, which is called a "bracelet," has still not been achieved and is the object of discussion in the literature. Naturally, in addition to linear structures we can expect shortly to hear about the synthesis of two-dimensional and three-dimensional structures from C_{60} and other fullerenes, the variety of whose physical and chemical properties can scarcely be predicted. Metallorganic compounds of the form $(C_{60}Pd)_n$, $(C_{60}Pd_2)_n$, and $(C_{60}Pd_3)_n$ have recently been synthesized.¹³⁷

Work directed toward obtaining fluorides of fullerenes is of great practical interest. This interest arises from the

prospect of creating compounds analogous to Teflon which can serve as the basis for lubricants with unique properties. Despite considerable experimental and theoretical activity in these studies,⁹⁵⁻¹⁰⁰ it is still premature to speak about a final verdict in this area. The announcement⁹⁵ regarding synthesis of fully fluorinated fullerene $C_{60}F_{60}$ was not confirmed by the results of subsequent experiments,^{96,97} where as the result of fluorination of the fullerene C_{60} and C_{70} the compounds $C_{60}F_{36}$ and $C_{70}F_{44}$ were synthesized. Even the preliminary experimental results^{96,97} show that such compounds are attractive as lubricants. On the other hand, the fully fluorinated fullerene $C_{60}F_{60}$ was found to be chemically unstable: under the action of water vapor intense production of HF occurs, accompanied by partial recovery of the fullerene fluoride.⁹⁸ Compounds of bromine with C_{60} have been obtained and described.¹³⁸

3.3. Soot and fullerenes

In the flame of burning organic compounds a complicated process of chemical transformation takes place as a result of which the final products are carbon dioxide and water. However, in the intermediate stage of these processes in a flame other clusters and radicals can be formed, including the C_{60} cluster (Refs. 101, 102). It is evident that these intermediate compounds affect the properties of the flame, since they determine the rate of chemical transformation and the energy balance in the flame. In particular, analysis of the optical properties of a candle flame^{103,104} shows that a significant part of the organic material in the intermediate stage of the process forms soot. In fact, the radiant power of a transparent flame is proportional to the mass of soot in it, and does not depend on the mass of the soot particles. Consequently, based on the measured parameters of a flame radiation we can estimate the mass of soot in the flame and compare it with the mass of the organic material taking part in the process. This comparison also shows that a substantial part of the organic material in the flame is in the form of soot particles, which are what produce the radiation.

These soot particles are produced in a candle flame in the chemical reaction in which molecules of the stearin $C_{18}H_{36}O$ participate. It is clear that such complex molecules can serve as the basis for the formation of clusters with a large number of atoms. Another conclusion is also possible: flames from organic compounds containing large molecules serve as a source of radiation. Flames of simple organic compounds (methane, alcohol) are characterized by a low light efficiency (the ratio of the brightness of the light to the thermal power), since in this case the rate of forming large clusters (soot particles producing radiation) is low.

If the soot particles in a flame are C_{60} clusters, then this will be reflected in the properties of the flame. These clusters have no allowed emitting transitions in the optical region of the spectrum, so a flame containing them will be less bright than in the presence of other soot particles. On the other hand, the radiation of the flame in the infrared region of the spectrum due to C_{60} clusters is very efficient, especially if vibrationally excited clusters form under non-

equilibrium conditions. If the flame properties depend on the rate of the chemical reaction in which carbon is oxidized, then the presence of C_{60} clusters slows down this process due to the chemical inertia of the cluster. Hence C_{60} clusters in a flame reduce its temperature.

Obviously, the way C_{60} clusters form in a flame is the same as under other conditions, including those in astrophysics.²⁴ This consists of adding new rings (pentagons or hexagons) to the elements of the cluster. As a result of this process various carbon clusters with closed shells can form, including C_{60} .

This analysis shows that the C_{60} cluster can be one of the varieties of soot present in a flame of organic compounds. In this case the flame properties differ from those which are produced by other flame particles. The presence of clusters in a flame can be detected from the emission of the flame in the 1429, 1183, 577, and 528 cm^{-1} lines, corresponding to the strongest transitions of the C_{60} cluster. The process of soot formation in a flame and its cluster structure have been studied in detail by Gerhardt *et al.*,¹⁰¹ who used a disk-shaped burner with diameter 75 mm in a chamber at reduced pressure. The object of the investigation was to study flames of benzene C_6H_6 and acetylene C_2H_2 burning under conditions in which the C/O ratio was varied. A cold mixture of the hydrocarbon and oxygen was fed into the burner at a temperature of 300 K and a pressure of 20 torr at a velocity varying from 35 to 60 cm/s. The burner terminated in an output orifice of diameter 0.8 mm, which served to form a supersonic stream of fuel. The flame propagated in a vacuum chamber in which pumps were used to maintain a pressure $\sim 10^{-3}$ torr. In order to extract ions from various points in the flame they used quartz probes coated with platinum. The ion mass spectrum was studied by means of a time-of-flight mass spectrometer.

Detailed studies revealed a high rate of carbon cluster formation with a cage structure even at distances of more than 2 mm from the boundary of the burner. Shown in Fig. 22 (Ref. 101) is a typical mass spectrum of the positive carbon cluster ions C_n^+ obtained in a benzene flame with a ratio C/O=0.76 when the fuel was fed into the burner at a velocity 42 cm/s, with the gas being extracted at 15 mm from the end edge of the burner. The mass spectrometer signal is shown in units of the concentration of the respective particles in the flame. Note that this spectrum differs considerably from that of the negatively charged clusters, among which the C_{50}^- and C_{82}^- clusters have the highest concentration, whereas the C_{60} cluster is the twentieth or thirtieth in concentration. The mass spectra of carbon clusters in acetylene and benzene flames have the same qualitative properties, although the acetylene flame is somewhat richer in the larger clusters than that of benzene.

As can be seen from the data shown in Fig. 22, the mass spectrum of the carbon clusters in hydrocarbon flames agree qualitatively with the mass spectrum of the clusters observed in connection with thermal vaporization of graphite (Fig. 10). One additional distinctive property of the cluster mass spectra is the absence of $C_{2n}H$ com-

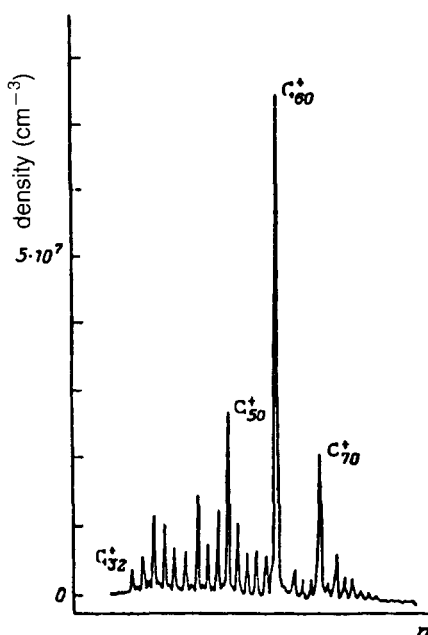


FIG. 22. Mass spectrum of the positive carbon cluster ions obtained in a benzene flame with the ratio $[C]/[O]=0.76$ when the fuel was fed into the burner at a velocity of 42 cm/s and the gas was extracted for the analysis at a distance of 15 mm from the edge of the burner.¹⁰¹

pounds. Only $C_{2n+1}H$ clusters, with an odd number of carbon atoms, contain hydrogen.

A good idea of the kinetics of clusterization and soot formation in a hydrocarbon flame can be derived from the results shown in Fig. 23, obtained by measuring the spatial dependence of the densities of various negatively charged carbon clusters in a benzene flame.¹⁰¹ As can be seen, the density of the C_{50}^- , C_{44}^- , and C_{82}^- clusters which acquired their largest values close to the edge of the burner, drop off sharply as a function of distance from the edge of the burner, although the density of the C_{60}^- clusters continues to increase monotonically as a function of distance from the end of the burner. This implies that the C_{44} , C_{60} and C_{82} clusters are the intermediate products of clusterization, whose final product is obviously the more stable C_{60} cluster.

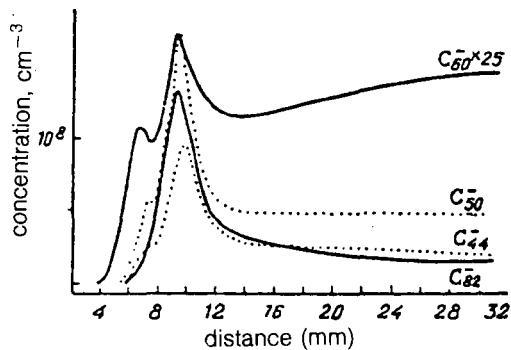


FIG. 23. Negative carbon ion cluster concentrations as a function of distance from the end of the burner in a benzene flame.¹⁰¹

Studies carried out by Gerhardt *et al.*¹⁰¹ imply that soot formation processes are very sensitive to temperature in hydrocarbon flames. Thus, raising the temperature by 200 K reduces the density of the positively charged clusters C_{60}^+ by approximately a factor of ten. The flame temperature corresponding to the maximum density of clusters with regular polyhedral structure is about 2100 K.

4. FULLERENES IN CONDENSED SYSTEMS

4.1. Structure of fullerenes

Condensed systems consisting of closed fullerene structures are usually called fullerites. Let us first consider a system of this sort consisting of C_{60} clusters. Since the interaction between the carbon atoms inside the C_{60} molecule is considerably stronger than that between atoms of different molecules, in the condensed system the individual C_{60} molecules must be regarded as inert, retaining their individuality when they interact with one another. Then the structure of the condensed system formed by such a way is similar to that of solid inert gases, since its structural elements are spherically symmetric atoms.

Thus we can expect that a condensed C_{60} system will have a close-packed structure similar to condensed inert gases. In a close-packed structure¹⁰⁸⁻¹¹¹ each molecule (or atom) has 12 nearest neighbors. There are two such structures: the face-centered cubic (fcc) lattice and the hexagonal close-packed (hcp) lattice, where the choice between the two is dependent on the details of the molecular interaction, and in particular can be determined by the conditions under which the crystal is grown.

Measurements show that for condensed carbon consisting of C_{60} clusters the hard-sphere model is applicable; it corresponds to close-packed structure. At temperatures on the order of room temperature both close-packed structures are observed, both fcc and hcp.¹¹²⁻¹¹⁹ The separation between nearest neighbors at room temperature according to these measurements is $a = 1.001 \pm 0.001$ nm, where the error is associated with the fact that the specimens were deposited on different substrates. This parameter is consistent with the density of the form of carbon in question, which is equal to

$$\rho = 2m/a^3 = 1.69 \pm 0.01 \text{ g/cm}^3.$$

We used the hard-sphere model for the structure of condensed carbon made up of C_{60} clusters. This is equivalent to using a pair potential interaction between individual clusters, where the various crystal parameters can be expressed in terms of the parameters of this interaction potential. To describe the actual situation correctly we must alter this model slightly. It is convenient to set the diameter of this sphere equal to the corresponding diameter of a cluster, i.e., the distance between diametrically opposite cluster atoms. The interaction potential should be treated as dependent on the distance between spheres. In accordance with the information given previously, the radius of the spheres is equal to 0.67 nm, so that the distance between spheres is approximately 0.33 nm.

Note that in a structure with close packing each sphere has 12 nearest neighbors, so that this structure would be optimum if the interaction between nearest neighbors occurred through pentagons. This would be true if the optimum interaction energy of two clusters corresponded to the situation in which their pentagons faced one another. However, the optimum configuration for the interaction of two C_{60} clusters is different: it occurs when the cluster hexagons face one another, with the centers of these hexagons displaced by 0.09 nm from one another.¹¹⁴ In this case the binding energy of two C_{60} clusters is 7.3 kcal/mol, which is greater than the energy per one cluster-cluster bond in the crystal, 6.1 kcal/mol.

Thus close packing is a rough approximation for a condensed system composed of C_{60} clusters. Calculations¹¹⁴ for a fcc lattice of such a crystal show that the 8 nearest neighbors of a test cluster interact with it almost optimally (i.e., contact is made through the hexagons), so that the interaction energy is 7.1 kcal/mol and the separation between the centers is 0.983 nm. The energy of interaction with the 4 other nearest neighbors is 6.1 kcal/mol and the equilibrium separation between them is equal to 1.006 nm.

Obviously, at high temperature the neighboring clusters, interacting with a test cluster in an optimal manner can be changed. This is caused by rotation of the cluster and tunnel transitions from one configuration to another. At low temperatures it is possible to have a phase transition, accompanied by the formation of a new structure. Note that with the numbers given above for the interaction energies of neighboring atoms this transition is energetically unfavorable, which reflects on their accuracy.

At a temperature of 252–259 K there is a first-order phase transition.^{120,121} At low temperatures a simple cubic (sc) lattice is stable; at high temperatures a fcc lattice is optimal. The phase transition is accompanied by a small change in the lattice constant. Thus, according to the measurements of Heiley *et al.*¹²² carried out using the x-ray techniques of neutron analysis, the lattice constant changes from 1.4154 ± 0.0003 nm to 1.4111 ± 0.0003 nm (i.e., by $4.3 \pm 0.6\%$) in the transition from a fcc lattice to a sc lattice (i.e., in freezing).

The measurements of David *et al.*¹²³ point to a cubic lattice structure at low temperatures. In this case the center of a pentagon of one of the clusters is located almost immediately above the middle of the line joining two hexagons of a neighboring cluster. Thus, it is easy to distinguish the points of the cluster with which it interacts with neighboring clusters. They correspond to intersection of the cluster with three mutually perpendicular axes passing through the cluster center, such that the intersection points are either pentagon centers or centers of the segments separating two hexagons.

It should be pointed out that in the phase transition the carbon density changes by almost 40%. This explains why it is easy to create intercalated compounds of this carbon form by inserting impurity atoms into the free places. In particular, this is how X_3C_{60} compounds (where X is an

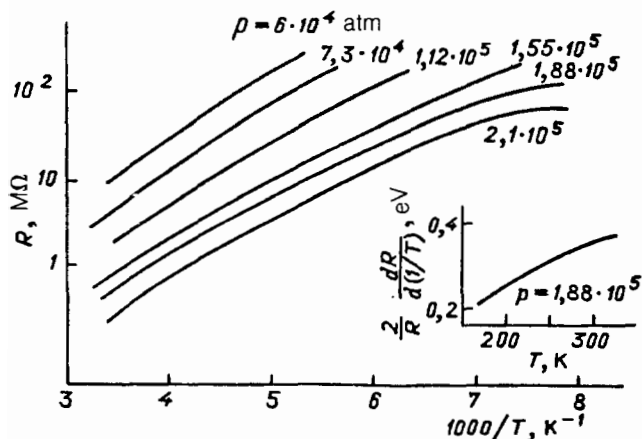


FIG. 24. Temperature dependence for the electrical resistance of a pure polycrystalline C_{60} sample of dimensions $0.3 \times 0.7 \times 0.04 \text{ mm}^3$, measured at different values as a function of the applied pressure.¹⁴³ In the lower right-hand corner the insert shows the temperature dependence of the logarithmic derivative of the resistance with respect to temperature at a pressure of $1.88 \cdot 10^5 \text{ atm}$, which characterizes the energy gap for the material.

alkali metal atom), which are superconductors, are produced.

The crystal structure of solid C_{70} near room temperature has been studied experimentally in detail.¹³⁹ The results of this work show that such crystals are characterized by body-centered cubic structure with a small admixture of the hexagonal phase.

4.2. Electrical properties of solid fullerenes

Solid fullerenes, sometimes called fullerites, are semiconductors for which the energy gap is 1.5–1.95 eV (Refs. 58, 141), 1.91 eV (C_{70}) (Ref. 142), and 1.2 eV (C_{84}) (Ref. 143). Detailed studies of how the properties of polycrystalline C_{60} samples vary as functions of temperature and pressure have been carried out.^{143–145} In our opinion, in the very profound work,¹⁴³ samples of pure C_{60} with dimensions $0.4 \times 0.7 \times 0.04 \text{ mm}^3$ were placed in an ampul of diameter 1 mm, where they were subjected to a pressure at various temperatures. The results of the measurements, shown in Fig. 24, reveal that the electrical resistance of the sample dropped by approximately a factor of ten when the pressure was increased to 10^5 atm . The temperature dependence deviated slightly from linearity, so that it is not possible to deduce unique values for the energy gap of the sample under these conditions. Some idea of the way the energy gap changes as a function of temperature can be derived from the temperature dependence of the logarithmic derivative of the resistivity with respect to $1/T$, shown in the lower part of Fig. 24. As can be seen, at high pressures the energy gap is several times smaller than the corresponding value under normal conditions.

Figure 25 shows the energy gap derived from the temperature dependence of the electrical resistance of various samples of polycrystalline C_{60} subjected to an external pressure. All samples had identical dimensions, given

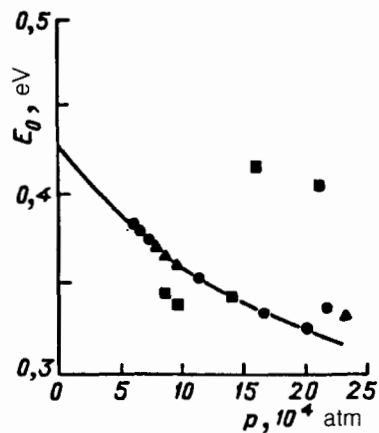


FIG. 25. The energy gaps of polycrystalline C_{60} obtained from temperature dependencies of the electric resistances of samples of various pressures. Different symbols correspond to different samples, and circles relate to samples of high purity.¹⁴³

above. The circular points correspond to samples with an elevated purity level. As can be seen, increasing the pressure to $2 \cdot 10^5 \text{ atm}$ monotonically reduces the electrical resistance. By analyzing the behavior of the highly purified sample we conclude that a further increase in the pressure would result in an increase in the energy gap that characterizes the sample. The temperature dependence of the energy gap shown in Fig. 24 can be explained in terms of thermal expansion of the sample, which has the same effect as reducing the pressure.¹⁴⁶ Localized states related to orientational disordering¹⁴³ can also play a definite role. The increase in the energy gap pressures above $2 \cdot 10^5 \text{ atm}$ implies the existence of a semiconductor–metal phase transition, predicted by Achiba *et al.*¹⁴² at pressures $\sim 2 \cdot 10^6 \text{ atm}$. Hence it is plausible to suppose that at elevated pressures a structure develops in solid carbon with covalent bonds between carbon atoms belonging to different C_{60} molecules, as is found in diamond.¹⁴³

Requeiro *et al.*¹⁴⁷ established that it is possible to form diamond crystal structure from polycrystalline C_{60} subjected to a pressure $\approx 2 \cdot 10^5 \text{ atm}$ at room temperature. They used the same apparatus as in the work cited above.¹⁴³ Note that in order to transform polycrystalline graphite into diamond it is necessary to subject it to a pressure $\sim (3-5) \cdot 10^6 \text{ atm}$ (Ref. 48).

Along with the energy gap the nature and time of the carrier relaxation are important properties of semiconducting materials. Detailed experiments have been performed to study this question,¹⁵⁰ where a C_{60} film of thickness $\sim 100 \text{ nm}$ deposited on a sapphire substrate was used as the object of these studies. The nature of the relaxation of the carriers formed when the film was irradiated with pulses from a neodymium laser with energy 0.2 nJ and repetition rate 100 MHz was analyzed on the basis of the results of measurements of the time dependence of the transparency of the film to radiation at $\lambda = 605 \text{ nm}$. The measurements showed that the relaxation is nonexponential and is described by the function

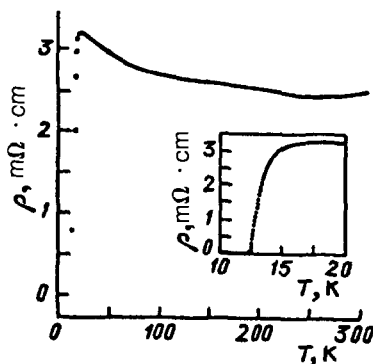


FIG. 26. Temperature dependence of the specific resistivity of a thin film of K_3C_{60} with the thickness $0.16 \mu\text{m}$ (Ref. 154).

$$F(t) = \exp[-(t/\tau)^\beta],$$

where the parameters $\beta = 0.4 \pm 0.05$ and $\tau = 48 \pm 7$ ns do not depend on the temperature when it varies in the range 150–400 K. This behavior of the carriers in relaxation implies that they are localized. The absence of temperature dependence in the carrier recombination time implies that recombination proceeds by a hopping mechanism involving a tunneling transition of electrons between localized states.

4.3. New superconductors

Interest in studying the electrical properties of solid fullerenes rose sharply after it was found early in 1991 that by doping solid C_{60} with a small quantity of alkali metal a material can be formed with metallic conductivity. At low temperatures it undergoes a transition to the superconducting state.^{20-22,151-153} This material is produced by processing films or polycrystalline samples of C_{60} with metal vapor at temperatures of several hundred degrees Celsius.¹⁵ The state with metallic conductivity corresponds to the X_3C_{60} structure, where X is an atom of the alkali metal. Figure 26 displays the temperature dependence of the resistivity of a K_3C_{60} film of thickness 160 nm deposited on a glass substrate.¹⁵⁴ As can be seen, the resistivity of polycrystalline C_{60} doped with potassium is about as low as eight orders of the corresponding value ($\sim 10^5 \Omega \cdot \text{cm}$) of pure C_{60} . The transition to the superconducting state is observed to occur in the temperature range 10–20 K.

Another important parameter characterizing the electrical properties of solid fullerenes with metallic conductivity is the Hall parameter. Figure 27 shows the results of measuring the temperature dependence of this parameter for a K_3C_{60} film of thickness approximately 160 nm deposited on a glass substrate.¹⁵⁴ Analysis of the data shown in Figs. 26 and 27 allows the basic properties of conducting solid fullerenes to be deduced. Thus, assuming that in K_3C_{60} there are three electrons in the conduction band per one (C_{60} molecule) and using the classical formula

$$\tau = m/\rho n e^2,$$

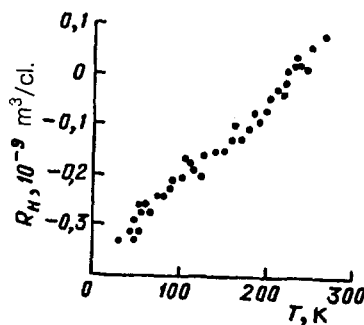


FIG. 27. Temperature dependence of the Hall parameter measured for a K_3C_{60} film of thickness $0.16 \mu\text{m}$ (Ref. 154).

where τ is the characteristic electron scattering time, m is the electron mass, and n is the electron density, we find $\tau = 3 \cdot 10^{-16}$ s. Palstra *et al.*¹⁵⁴ explain the relatively low conductivity of K_3C_{60} in terms of the fine-grain structure of this film, which is shown by measurements to consist of granules of dimension 6–8 nm. The change in the sign of the Hall parameter as a function of temperature implies that the sign of the principal carriers changes, i.e., there is a transition from an electron conductivity mechanism to a hole mechanism. This transition is characteristic of a half-filled conduction band; it is completely filled in K_6C_{60} .

The solid compound K_3C_{60} , which has metallic conductivity, begins to undergo the transition to the superconducting state at $T = 19$ K. This value of the critical temperature is the highest ever found for molecular superconductors. Thus, the critical temperature characterizing superconductivity in graphite intercalated with potassium is 0.55 K (Ref. 155). The superconductivity of K_3C_{60} was observed not only in films but also in polycrystalline samples.

Figure 28 displays the results of measuring the temperature dependence of the specific magnetization of a K_3C_{60} superconducting sample, performed using a SQUID magnetometer.²⁰ The sample was prepared by means of a chemical reaction of 29.5 mg C_{60} with 4.8 mg K taking place over 36 h at $T = 200^\circ\text{C}$. The sample was cooled with (FC) and without (ZFC) a magnetic field. The shape of

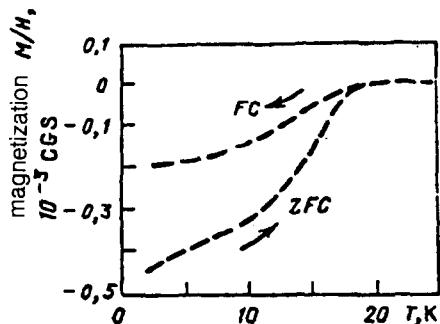


FIG. 28. Temperature dependence of the specific magnetization of a superconducting K_3C_{60} sample.²⁰ The sample was cooled with (FC) and without (ZFC) a magnetic field.

TABLE V. Superconducting critical temperatures T_c , lattice constant a_0 , and fraction of the structure represented by fcc for polycrystalline X_3C_{60} or XY_2C_{60} samples.¹⁵⁶ The two Na_2CsC_{60} samples differ in the way in which they were prepared.

Material	T_c , %	a_0 , nm	Volume fraction fcc, %
$RbCs_2C_{60}$	33	$1,4555 \pm 0,0007$	60
Rb_2CsC_{60}	31	$1,4431 \pm 0,0006$	60
Rb_3C_{60}	29	$1,4384 \pm 0,0010$	70
KRb_2C_{60}	27	$1,4323 \pm 0,0010$	84
K_2CsC_{60}	24	$1,4292 \pm 0,0010$	60
K_2RbC_{60}	23	$1,4243 \pm 0,0010$	75
K_3C_{60}	19	$1,4240 \pm 0,0006$	70
Na_2CsC_{60}	12	$1,4134 \pm 0,0006$	72
Li_2CsC_{60}	12	$1,4120 \pm 0,0021$	1
Na_2RbC_{60}	2,5	$1,4028 \pm 0,0011$	2
Na_2KC_{60}	2,5	$1,4025 \pm 0,0010$	0,1
Na_2CsC_{60}	12	—	36
Na_2CsC_{60}	12	—	6
C_{60}		$1,4161 \pm 0,0009$	

the curves implies the presence of a strong Meissner effect, which is evidence for the superconductivity of the sample at temperatures below 18 K.

Shortly after the discovery of superconductivity in the solid fullerene K_3C_{60} it was found that almost all solid fullerenes obtained by intercalating alkali metal atoms in the C_{60} crystal structure in stoichiometric proportions to make either X_3C_{60} or XY_2C_{60} (here X and Y are alkali metal atoms) possess superconducting properties. Table V shows the results of the most complete comparative study of superconducting compounds of this type, carried out by Tanigaki *et al.*¹⁵⁶ The values of the critical temperature were determined from the temperature dependence of the magnetization of polycrystalline samples. The measurements were made using a SQUID magnetometer, cooling the sample when the magnetic field was turned on and when it was turned off. As shown by the data presented in the table, a correlation (noted even in early work^{143,157}) between the value of the parameter a_0 characterizing the fcc lattice and the superconductivity critical temperature is observed. The volume fraction of fcc structure in the sample was determined by the x-ray diffraction technique.

The correlation between the lattice constant a_0 and the critical temperature of superconducting fullerenes can be seen most distinctly from Fig. 29. Here $\ln T_c$ is plotted as a function of $N^{-1}(E_F)$ the reciprocal of the energy density of the electron states at the Fermi level.^{143,157} This quantity is proportional to the lattice constant a_0 which characterizes the fcc structure. The linear behavior of this dependence implies a phonon mechanism for the superconductivity in fullerenes. In fact, it follows from the BCS superconductivity model that the superconductivity critical temperature T_c is given in terms of the parameters of the superconducting material by

$$T_c = \omega_{ph} \exp\{-[VN(E_F)]^{-1}\} \quad (5)$$

where ω_{ph} is the phonon energy corresponding to the superconductive electron pairing, and V is a constant that characterizes the electron-phonon interaction energy

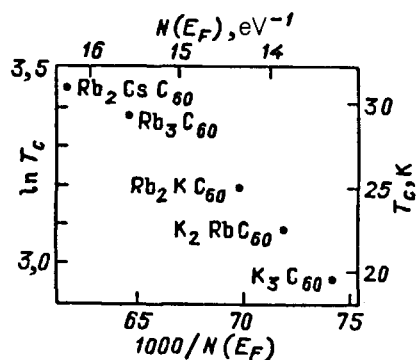


FIG. 29. Superconducting critical temperature of solid fullerenes doped with atoms of alkali metals as a function of the reciprocal of the energy density of the electron states $N(E_F)$ at the Fermi level.^{143,157}

which leads to electron pairing. The linear behavior of the dependence shown in Fig. 29 agrees with expression (5) under the conditions if the phonon frequency $\omega_{ph} \approx 300$ K and the electron-phonon interaction energy $V \approx 0.03$ eV are independent of the species of intercalated atom. This implies that intramolecular vibrations of C_{60} dominate in the electron pairing mechanism responsible for superconductivity.

Another experimental fact supports the decisive role of the phonon pairing mechanism for electron pairing in the superconductivity of fullerenes doped with alkali metals. This is the recently¹⁵⁸ measured pressure dependence of the K_3C_{60} superconductivity temperature. The results of the measurements, performed on two samples prepared in different ways, are shown in Fig. 30. It can be seen that the value of T_c drops off almost linearly as a function of pressure. The characteristic slope of this dependence at low pressures is approximately equal to -0.78 K/kbar. Noting that the linear compressibility of the C_{60} fullerite is $d \ln a_0 / dp = 2.3 \cdot 10^{-12}$ cm²/dyne (Ref. 159), we find that the dependence of T_c on pressure can be interpreted as a dependence on the lattice constant a_0 , where the coefficient dT_c / da_0 is approximately equal to 2.36 K/nm. This is somewhat less than the value dT_c / da_0 which can be extracted from the data shown in Table V. However, the

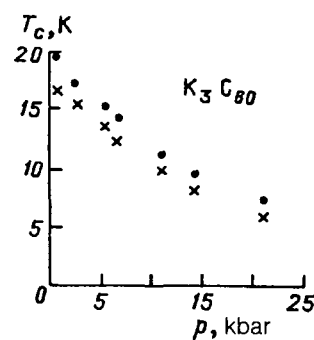


FIG. 30. Superconductivity transition temperature of two K_3C_{60} samples prepared in different ways as a function of the applied pressure.¹⁵⁸

agreement between these values in order of magnitude implies the common nature of dependencies of T_c on pressure and the fcc lattice constant, and supports the view that the phonon superconductivity mechanism dominates. This also agrees with the results of measuring T_c as a function of applied pressure for Rb_3C_{60} (Ref. 159), according to which $dT_c/dp \approx -1$ K/kbar. It agrees with the value of the slope $dT_c/da_0 \approx 3$ K/nm, which differs even less from the corresponding value derived from the data of Table V.

The electron pairing mechanism responsible for the occurrence of superconductivity in materials on the basis of C_{60} is the object of the most intensive study. In a series of recent papers, in addition to the phonon formation mechanism for Cooper pairs,^{160,162} a purely electron pairing mechanism has also been studied in detail.^{163,164} A reliable conclusion regarding the superconductivity mechanism can be drawn based on the experimental study of the isotopic dependence of the Curie temperature T_c corresponding to the transition of the material to the superconducting state. For the phonon superconductivity mechanism the isotopic dependence of T_c is given by

$$T_c \sim M^{-\alpha}, \quad (6)$$

where M is the isotope mass and $\alpha < 0.5$. For the electron mechanism of electron pairing the T_c has essentially no isotopic dependence. The experimental investigation of the isotope effect for the superconductor Rb_3C_{60} (Ref. 165) showed that T_c dropped by 0.65 ± 0.10 K when ^{12}C was replaced with ^{13}C . This is $75 \pm 5\%$ of the change determined by relation (6) for $\alpha = 0.5$. Analysis of the results of this experiment in conjunction with Eq. (6) leads to the value $\alpha = 0.37 \pm 0.05$. This implies that the electron-phonon interaction makes the principal contribution to the superconductivity mechanism, with some influence of Coulomb interaction effects which reduce the value of α . Ramirez *et al.*¹⁶⁵ used a polycrystalline sample of Rb_3C_{60} containing the isotope ^{13}C in abundance $90 \pm 5\%$. The isotopic dependence of T_c was determined by comparing the temperature dependences of the magnetization obtained for magnetic fields of 5 and 10 G.

These experimental results do not contradict the data recently obtained in studies of the isotope effect in the superconductivity of K_3C_{60} (Ref. 166). The distinctive feature in this experiment is associated with the use of the isotope ^{13}C and with a level of enrichment 99%. The superconducting temperature of the isotope-substituted K_3C_{60} dropped from 19.2 to 18.8 K, which agrees with the value of the parameter $\alpha = 0.3 \pm 0.06$ that goes into expression (6). A detailed survey of the work on the electrical properties and superconductivity of fullerenes doped with alkali metals was given by Haddon *et al.*¹⁴⁰

4.4. Optical properties of materials on the basis of fullerenes

Single-crystal C_{60} is a semiconductor whose energy gap is ~ 1.5 eV. It follows that photoconductivity of solid C_{60} can be observed under irradiation by visible light. The phenomenon of photoconductivity, whose use would substantially broaden the range of potential applications for

fullerenes, was observed by Wang.¹⁶⁷ A film made of polyvinylcarbazol (PVC) with molecular weight $\sim 5 \cdot 10^5$ was saturated with a mixture of $\text{C}_{60} + \text{C}_{70}$ in the ratio 85:15, dissolved in 12 ml of toluene. There was approximately 40 mg of fullerenes for 1.5 g of PVC. The solution was dried out on an aluminum substrate at $T \approx 400$ K over several hours. The thickness of the resulting film varied from 1 to 30 μm . The optically transparent films thus obtained remained stable for several months. To measure the photoconductivity of the films they used the conventional technique, based on a photo-induced discharge. The film on the grounded aluminum substrate was first charged positively or negatively by means of a corona discharge in darkness. Photoelectrons and holes that formed in the bulk of the film as a result of irradiation diffused toward the surface, where they underwent recombination with charged particles of the opposite sign. This was detected with an electrostatic voltmeter. The measurements showed that the photoabsorption spectrum of PVC with an admixture of fullerenes occupies the range from 280 to 680 nm. The quantum yield with respect to the formation of electron-ion pairs was 0.9. These parameters permit us to conclude that this material is among the best organic superconductors.

The favorable prospects for using fullerenes in optical materials are confirmed by the results of measurements recently performed on the nonlinear optical properties of a C_{60} film.¹⁶⁸ These measurements showed that when linearly polarized laser radiation with wavelength $\lambda = 1064$ nm passed through a C_{60} film of thickness 60 nm oriented in a certain direction sputtered onto a silicon substrate, doubling and tripling of the frequency was observed. The results of the measurements show that the magnitude of the third-order nonlinear optical susceptibility is equal to $|\chi_{1111}(-3\omega, \omega, \omega, \omega)| = 2 \cdot 10^{-10}$ cgse, which puts fullerenes in one of the leading places among molecular nonlinear optical materials.

The nonlinear optical properties of fullerenes open up possibilities for employing them as optical shutter to limit the intensity of laser radiation. This possibility is based on the results of a recently performed experiment,¹⁶⁹ in which a decrease in the transparency of solutions of C_{60} and C_{70} in methylene chloride and toluene was demonstrated. The radiation source consisted of pulses of length 8 ns at the second harmonic $\lambda = 532$ nm of a neodymium laser. Figure 31 shows the output intensity of the laser radiation which has passed through the solution of C_{60} in toluene as a function of the intensity of the incident radiation, measured for two solutions which differ in the values of the transparency for low intensities of the incident radiation. It can be seen that the solution which has a transparency of 63% limits the intensity of the transmitted radiation to the value $\sim 10^7$ W/cm², while the solution with transparency 80% has a threshold radiation intensity which is higher by about an order of magnitude. The threshold intensity of the solution of C_{70} in toluene with a transparency of 70% is of about the same magnitude. The threshold intensity which characterizes an optical shutter made from fullerene solutions is several times lower than the corresponding value

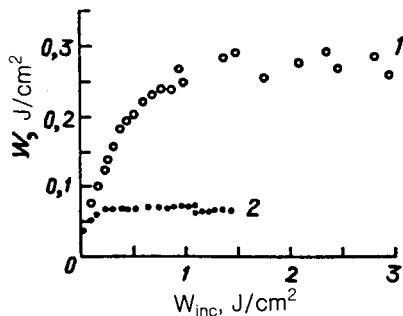


FIG. 31. Transmitted intensity as a function of the incident radiation flux, measured using a solution of C_{60} in toluene with a transparency of 63% (1) and 80% (2) as a filter. The laser radiation had wavelength 532 nm and pulse length 8 ns.¹⁶⁹

for materials customarily used for these purposes (indantron, phthalocyanin chloralumina, etc.). This means that one can expect nonlinear optical components to be fabricated from C_{60} for optical digital processes, and also to protect optical sensors from intense radiation. The physical principle underlying the mechanism of an optical shutter made from fullerenes is related to the fact that when a C_{60} or C_{70} molecule absorbs a photon of wavelength $\lambda = 532$ nm the molecule is in a triplet state, which is characterized by an absorption cross section for this photon which is several times as large as the corresponding value for an unexcited molecule.

5. CONCLUSION

Fullerenes, whose existence was established in the mid-1980s, and for which an efficient separation technique was developed in 1990, have now become the object of intensive studies by dozens of scientific groups. Commercial firms are intently following the results of these studies. Since this form of carbon has already delivered a number of surprises to scientists, it would be pointless to discuss trends and possible implications of the study of fullerenes over the next decade, but we should be ready for new surprises.

In this connection it is useful to consider the philosophical side of the problem. In essence, fullerenes are an artificial material. Although they exist in the atmosphere and possibly even in interstellar space, the decisive role in the discovery was played by fundamental investigations of clusters. Specifically, fundamental studies led to the idea that there might be new carbon structures and the development of this concept resulted in a sophisticated technique for producing these materials which have such unique properties. Evidently, this process of innovation through fundamental scientific studies is a characteristic element in the development of future technologies based on refined scientific techniques and using leading-edge scientific information. Thus, the story of the discovery and study of fullerenes is instructive and gives us a useful example of the relationship with fundamental studies. We will await new surprises from fullerenes.

- ¹E. Osawa, *Kogaku* (Kyoto) **25**, 854 (1970).
- ²Z. Ioshida and E. Ozawa, *Aromaticity* (Kyoto) (1971).
- ³D. A. Bochvar and E. G. Gal'perin, *Dokl. Akad. Nauk SSSR* **209**, 610 (1973).
- ⁴I. V. Stankevich, M. V. Nikerov, and D. A. Bochvar, *Usp. Khim.* **53**, 640 (1984).
- ⁵R. A. Davidson, *Theor. Chim. Acta.* **58**, 193 (1984).
- ⁶A. D. J. Haymet, *J. Am. Chem. Soc.* **108**, 319 (1986).
- ⁷H. W. Kroto *et al.*, *Nature* **318**, 162 (1985).
- ⁸Q. L. Zhang *et al.*, *J. Phys. Chem.* **90**, 525 (1986).
- ⁹A. Kaldor *et al.*, *Zs. Phys.* **3**, 195 (1986).
- ¹⁰A. O'Keefe, M. M. Ross, and A. P. Baronavski, *Chem. Phys. Lett.* **130**, 17 (1986).
- ¹¹M. Y. Hahn *et al.*, *ibid.*, p. 12.
- ¹²S. C. O'Brien *et al.*, *ibid.*, **132**, 99; *J. Chem. Phys.* **88**, 220 (1988).
- ¹³D. M. Cox, K. C. Reichmann, and A. Kaldor, *J. Am. Chem. Soc.* **10**, 1588 (1988).
- ¹⁴D. S. Bethune *et al.*, *Chem. Phys. Lett.* **179**, 219 (1990).
- ¹⁵G. Meijer and D. S. Bethune, *J. Chem. Phys.* **93**, 7800 (1990).
- ¹⁶R. D. Johnson, G. Meijer, and D. S. Bethune, *J. Am. Chem. Soc.* **112**, 8983 (1990).
- ¹⁷W. Krätschmer *et al.*, *Nature* **347**, 354 (1990).
- ¹⁸W. Krätschmer, K. Fostiropoulos, and D. R. Huffman, *Chem. Phys. Lett.* **170**, 167 (1990).
- ¹⁹W. Krätschmer, K. Fostiropoulos, and D. R. Huffman, in *Dusty Objects in the Universe*, E. Bussoletti and A. A. Cittone (eds.), Kluwer (1990).
- ²⁰A. F. Hebard *et al.*, *Nature* **350**, 600 (1991).
- ²¹H. Holczer *et al.*, *Science* **252**, 1154 (1991).
- ²²M. J. Rosseinsky *et al.*, *Phys. Rev. Lett.* **66**, 2830 (1991).
- ²³H. H. Wang *et al.*, *Inorg. Chem.* **30**, 2838 (1991).
- ²⁴H. Kroto, *Science* **242**, 1139 (1988).
- ²⁵R. E. Smalley, *Acc. Chem. Res.* **25**, 98 (1992).
- ²⁶H. W. Kroto, A. W. Allaf, and S. P. Balm, *Chem. Rev.* **91**, 1213 (1991).
- ²⁷R. F. Curl and R. E. Smalley, *Sci. Am.* **265**, 54 (1991).
- ²⁸R. E. Smalley, *The Sciences* **31**, 22 (1991).
- ²⁹A. V. Eletskii and B. M. Smirnov, *Usp. Fiz. Nauk* **161**, 173 (1991) [*Sov. Phys. Usp.* **34**, 274 (1991)].
- ³⁰E. E. Flint, *Beginning Crystallography* [in Russian], Vysshaya Shkola, Moscow (1961).
- ³¹V. S. Veselovskii, *Graphite* [in Russian], Moscow (1960).
- ³²W. I. F. David *et al.*, *Nature* **353**, 147 (1991).
- ³³K. Hedberg *et al.*, *Science* **254**, 410 (1991).
- ³⁴J. M. Hawkins, *et al.*, *ibid.* **252**, 213.
- ³⁵R. Taylor *et al.*, *J. Chem. Soc. Chem. Comm.* 1423 (1990).
- ³⁶D. R. McKenzie *et al.*, *Nature* **355**, 622 (1992).
- ³⁷R. Ertl *et al.*, *ibid.* **353**, 149 (1991).
- ³⁸G. Von Helden *et al.*, *J. Chem. Phys.* **95**, 3835 (1991).
- ³⁹H. W. Kroto *et al.*, *Nature* **90**, 529 (1987).
- ⁴⁰J. P. Hare, H. W. Kroto, and R. Taylor, *Chem. Phys. Lett.* **177**, 394 (1991).
- ⁴¹R. E. Haufler *et al.*, *J. Phys. Chem.* **94**, 8634 (1990).
- ⁴²Gu Zhennan *et al.*, *ibid.* **95**, 9615 (1991).
- ⁴³T. Pradeep and C. N. Rao, *Mat. Res. Bull.* **26**, 1101 (1991).
- ⁴⁴F. Diederich *et al.*, *Science* **252**, 548 (1991).
- ⁴⁵I. G. Dance *et al.*, *J. Phys. Chem.* **95**, 8425 (1991).
- ⁴⁶J. D. Brooks and G. H. Taylor, *Carbon* **3**, 185 (1965); *Nature* **206**, 697 (1965); *Chem. Phys. Carbon* **4**, 243 (1968).
- ⁴⁷D. R. Huffman *Phys. Today*, November, 22 (1991).
- ⁴⁸Z. Slanina *et al.*, *J. Mol. Struct. THEOCHEM.* **202**, 169 (1989).
- ⁴⁹D. E. Weeks and W. G. Harter, *J. Chem. Phys.* **90**, 4744 (1989).
- ⁵⁰R. E. Stanton and M. D. Newton, *J. Phys. Chem.* **92**, 2141 (1988).
- ⁵¹S. J. Cyvin *et al.*, *Chem. Phys. Lett.* **143**, 377 (1988).
- ⁵²Z. C. Wu, D. A. Jelski, and T. F. George, *ibid.* **137**, 291 (1987).
- ⁵³R. L. Cappelletti *et al.*, *Phys. Rev. Lett.* **66**, 3261 (1991).
- ⁵⁴K. Prassides *et al.*, *Chem. Phys. Lett.* **187**, 455 (1991).
- ⁵⁵C. Coulombeau *et al.*, *J. Phys. Chem.* **96**, 22 (1992).
- ⁵⁶F. Negri, G. Orlandi, and F. Zerbetto, *Chem. Phys. Lett.* **144**, 31 (1988).
- ⁵⁷D. S. Bethune *et al.*, *ibid.* **179**, 181 (1991).
- ⁵⁸H. Ajie *et al.*, *J. Phys. Chem.* **94**, 8630 (1990).
- ⁵⁹P. P. Radi *et al.*, *J. Chem. Phys.* **88**, 2809 (1988).
- ⁶⁰K. Raghavachari and S. Binkey, *J. Chem. Phys.* **87**, 2192 (1987).
- ⁶¹F. D. Weise *et al.*, *J. Am. Chem. Soc.* **110**, 4464 (1988).

- 62 P. P. Radi *et al.*, *Chem. Phys. Lett.* **174**, 223 (1990).
- 63 P. P. Radi *et al.*, *J. Chem. Phys.* **92**, 4817 (1990).
- 64 P. Wurz *et al.*, *J. Appl. Phys.* **70**, 6647 (1991).
- 65 K. R. Lykke and P. Wurz, *J. Phys. Chem.* **96**, 3191 (1992).
- 66 R. K. Yoo, B. Ruscic, and J. Berkowitz, *J. Chem. Phys.* **96**, 911 (1992).
- 67 D. Ben-Amotz *et al.*, *Chem. Phys. Lett.* **183**, 149 (1991).
- 68 D. R. Luffer and K. H. Schram, *Rapid Comm. Mass Spectr.* **4**, 555 (1990).
- 69 R. J. Doyle and M. M. Ross, *J. Phys. Chem.* **95**, 4954 (1991).
- 70 J. F. Christian, Z. Wan, and S. L. Anderson, *ibid.* **96**, 3574 (1992).
- 71 R. D. Beck *et al.*, *ibid.* **95**, 8402 (1991).
- 72 S. W. McElvany and M. M. Ross, *Mater. Res. Soc. Proc.* **206**, 607 (1991).
- 73 R. C. Mowrey *et al.*, *J. Chem. Phys.* **95**, 7138 (1991).
- 74 H.-G. Bushmann, Th. Lill, and I. V. Hertel, *Chem. Phys. Lett.* **187**, 459 (1991).
- 75 J. R. Heat *et al.*, *J. Am. Chem. Soc.* **107**, 7779 (1985).
- 76 F. D. Weise *et al.*, *ibid.* **110**, 4464 (1988).
- 77 D. M. Cox *et al.*, *ibid.* **108**, 2457 (1986).
- 78 L. M. Roth *et al.*, *ibid.* **113**, 6298 (1991).
- 79 T. Weisske, D. K. Bohme, and H. Schwarz, *J. Phys. Chem.* **95**, 8451 (1991).
- 80 T. Weisske, *et al.*, *Angew. Chem. Int. Ed. Engl.* **30**, 884 (1991).
- 81 M. M. Ross and J. H. Callahan, *J. Phys. Chem.* **95**, 5720 (1991).
- 82 T. Weisske *et al.*, *Chem. Phys. Lett.* **186**, 154 (1991).
- 83 J. Millican *et al.*, *Chem. Mater.* **3**, 386 (1991).
- 84 H. S. Chen *et al.*, *Appl. Phys. Lett.* **59**, 2956 (1991).
- 85 J. N. J. Ong, *Carbon* **2**, 281 (1964).
- 86 M. D. Newton and R. E. Stanton, *J. Am. Chem. Soc.* **108**, 2469 (1986).
- 87 G. H. Kroll *et al.*, *Chem. Phys. Lett.* **181**, 112 (1991).
- 88 F. Wudl, *Acc. Chem. Res.* **25**, 157 (1992).
- 89 J. R. Morton *et al.*, *J. Phys. Chem.* **96**, 3576 (1992).
- 90 J. M. Hawkins *et al.*, *J. Org. Chem.* **55**, 6250 (1990).
- 91 J. M. Hawkins, *Acc. Chem. Res.* **25**, 150 (1992).
- 92 P. J. Fagan, J. C. Calabrese, and B. Malone, *ibid.* **134**.
- 93 P. J. Fagan, J. C. Calabrese, and B. Malone, *Science* **252**, 1160 (1991); *J. Am. Chem. Soc.* **113**, 9408 (1991).
- 94 A. L. Balch, V. J. Catalano, and J. W. Lee, *Inorg. Chem.* **30**, 3980 (1991).
- 95 J. H. Holloway *et al.*, *J. Chem. Soc., Chem. Commun.* 966 (1991).
- 96 H. Selig *et al.*, *J. Am. Chem. Soc.* **113**, 5475 (1991).
- 97 J. E. Fischer, P. A. Heyney, and A. B. Smith, *Acc. Chem. Res.* **25**, 112 (1992).
- 98 R. Taylor *et al.*, *Nature* **355**, 27 (1992).
- 99 G. E. Scuseria, *Chem. Phys. Lett.* **176**, 423 (1991).
- 100 B. I. Dunlap *et al.*, *J. Phys. Chem.* **95**, 5763 (1991).
- 101 P. H. Gerhardt, S. Loffer, and K. H. Homann, *ibid.* 306.
- 102 B. D. Crittenden and R. Long, *Combust Flame* **20**, 359 (1973).
- 103 L. A. Luizova, B. M. Smirnov, and A. D. Khakhaev, *Dokl. Akad. Nauk SSSR* **309**, 1359 (1989) [*Sov. Phys. Dokl.* **34**, 1086 (1989)].
- 104 L. A. Luizova *et al.*, *Teplofiz. Vys. Temp.* **28**, 897 (1990).
- 105 A. L. Mackay, *Acta Crystallogr.* **15**, 916 (1962).
- 106 O. Echt, K. Satler, and E. Recknagel, *Phys. Rev. Lett.* **47**, 1121 (1981).
- 107 B. Raoult, J. Farges, M. F. deFeraudy, and G. Torchet, *Phil. Mag.* **60B**, 881 (1989).
- 108 C. Kittel, *Introduction to Solid State Physics*, 2nd ed., Wiley, New York (1956).
- 109 G. Liebfried, *Macroscopic Theory of Mechanical and Thermal Properties of Crystals* [Russian translation], GIFML, Moscow (1963).
- 110 C. Bann, *Crystals* [Russian translation], Mir, Moscow (1979).
- 111 N. W. Ashcroft and N. D. Mermin, *Solid State Physics*, Holt Rinehard & Winston, New York (1976).
- 112 W. Krätschmer, L. D. Lamb, K. Fostiropoulos, and D. R. Huffman, *Nature* **347**, 354 (1990).
- 113 R. J. Wilson, G. Meijer, D. S. Bethune, *et al.*, *Nature* **348**, 621 (1990).
- 114 Y. Guo, N. Krasawa, and W. A. Goddard, *Nature* **351**, 464 (1990).
- 115 V. P. Dravid, S. Liu, and M. M. Kappes, *Chem. Phys. Lett.* **185**, 75 (1991).
- 116 D. Schmicker, S. Schmidt, J. G. Skofronick, *et al.*, *Phys. Rev.* **44B**, 10995 (1991).
- 117 Y. Saito, N. Suzuki, H. Shinohard, and Y. Ando, *Jpn. J. Appl. Phys.* **30**, 2857 (1991).
- 118 J. Q. Li, X. Z. Zhao, D. B. Zhu, *et al.*, *Appl. Phys. Lett.* **59**, 3108 (1991).
- 119 T. Ichihashi, K. Tanigaki, T. W. Ebbesen, *et al.*, *Chem. Phys. Lett.* **190**, 179 (1992).
- 120 P. A. Heiley, J. F. Fischer, and A. R. McGhie, *Phys. Rev. Lett.* **66**, 2911 (1991).
- 121 J. S. Tse, D. D. King, and D. A. Wilkinson, *Chem. Phys. Lett.* **183**, 378 (1991).
- 122 P. A. Heiley, G. B. M. Vaughan, J. F. Fischer, *et al.*, *Phys. Rev. Lett.* **45B**, 4544 (1992).
- 123 W. I. F. David, R. H. Ibberson, J. C. Matthewman, *et al.*, *Nature* **353**, 147 (1991).
- 124 S. Lijima, *Nature* **354**, 56 (1991).
- 125 *Nature* **354**, 18 (1991).
- 126 A. L. Mackay and H. Terrones, *ibid.* **352**, 762 (1991).
- 127 S. Lijima, T. Ichihashi, and Y. Ando, *ibid.* **356**, 776 (1992).
- 128 T. W. Ebbesen and P. M. Ajayan, *ibid.* **358**, 220 (1992).
- 129 J. W. Motmire, B. I. Dunlap, and C. T. White, *Phys. Rev. Lett.* **68**, 631 (1992).
- 130 N. Hamada, S. Sawada, and A. Oshyama, *ibid.* p. 1579.
- 131 P. Calvert, *Nature* **357**, 365 (1992).
- 132 K. S. Khemani, M. Prato, and F. Wudl, *J. Org. Chem.* **57**, 3254 (1992).
- 133 K. Chatterjee *et al.*, *ibid.*, p. 3253.
- 134 D. M. Cox *et al.*, in *Fullerenes*, G. S. Hummond and V. J. Kuck (eds.), Am. Chem. Soc. Publ., Washington (1992); (ACS Symp. Ser. Vol. 481).
- 135 R. Malhotra, *ibid.*, p. 127.
- 136 R. E. Smalley, *ibid.*, p. 141.
- 137 L. F. Lindoy, *Nature* **357**, 443 (1992).
- 138 P. R. Birkett *et al.*, *ibid.*, p. 479.
- 139 G. B. M. Vaughan *et al.*, *Science* **254**, 1350 (1991).
- 140 R. C. Haddon *et al.*, in *Fullerenes*, G. S. Hummond and V. J. Kuck, Am. Chem. Soc. Publ., Washington (1992) (ACS Symp. Ser. V).
- 141 S. Saito and A. Oshiyama, *Phys. Rev. Lett.* **66**, 2637 (1991).
- 142 Y. Achiba *et al.*, *Chem. Lett.* 1233 (1991).
- 143 K. Kikuchi *et al.*, *ibid.*, p. 1607.
- 144 S. J. Duclos *et al.*, *Nature* **351**, 380 (1991).
- 145 M. N. Requeiro *et al.*, *ibid.* **354**, 289.
- 146 P. A. Heiney *et al.*, *Phys. Rev. Lett.* **66**, 2911 (1991).
- 147 N. M. Requeiro *et al.*, *Nature* **355**, 237 (1992).
- 148 P. Ball, *ibid.*, p. 205.
- 149 B. C. Guo, K. P. Kerns and A. M. Castleman, Jr., *Science* **255**, 1411 (1992); **256**, 515.
- 150 R. A. Cheville and N. J. Halas, *Phys. Rev. B* **45**, 4548 (1992).
- 151 R. C. Haddon *et al.*, *Nature* **350**, 320 (1991).
- 152 R. C. Haddon, *Acc. Chem. Res.* **25**, 127 (1992).
- 153 H. H. Wang *et al.*, *Inorg. Chem.* **30**, 2838 (1991).
- 154 T. T. M. Palstra *et al.*, *Phys. Rev. Lett.* **68**, 1054 (1992).
- 155 N. B. Hannay *et al.*, *ibid.* **14**, 225 (1965).
- 156 K. Tanigaki *et al.*, *Nature* **356**, 419 (1992).
- 157 R. M. Fleming *et al.*, *ibid.* **352**, 787 (1991).
- 158 G. Sparr *et al.*, *Science* **252**, 1829 (1991).
- 159 J. E. Fisher *et al.*, *ibid.*, p. 1288.
- 160 C. M. Varma, J. Zaanen, and K. Raghavachari, *ibid.* **254**, 989.
- 161 M. A. Schluter *et al.*, *Phys. Rev. Lett.* **68**, 526 (1992).
- 162 F. C. Zhang, M. Ogato, and T. M. Rice, *ibid.* **67**, 3452.
- 163 S. Chakravarty, G. Kivelson, and M. P. Gelfand, *Science* **254**, 970 (1991).
- 164 G. Baskaran and E. Tossati, *Curr. Sci.* **61**, 33 (1991).
- 165 A. P. Ramirez *et al.*, *Phys. Rev. Lett.* **68**, 1058 (1992).
- 166 C.-C. Chen and C. M. Lieber, *J. Am. Chem. Soc.* **114**, 3141 (1992).
- 167 Y. Wang, *Nature* **356**, 585 (1992).
- 168 H. Hoshi *et al.*, *Jpn. J. Appl. Phys.* **L1397** (1991).
- 169 L. W. Tutt and A. Kost, *Nature* **356**, 225 (1992).

Translated by D. L. Book